AD-A164 636 THE NEUTRAL/ION CHEMISTRY OF SODIUM IN THE STRATOSPHERE 1/1
AND MESOSPHERE (U) ATMOSPHERIC AND ENVIRONMENTAL
RESEARCH INC CAMBRIDGE MA J M RODRIGUEZ ET AL.
UNCLASSIFIED 30 SEP 85 SCIENTIFIC-2 AFGL-TR-85-0237 F/G 4/1 NL

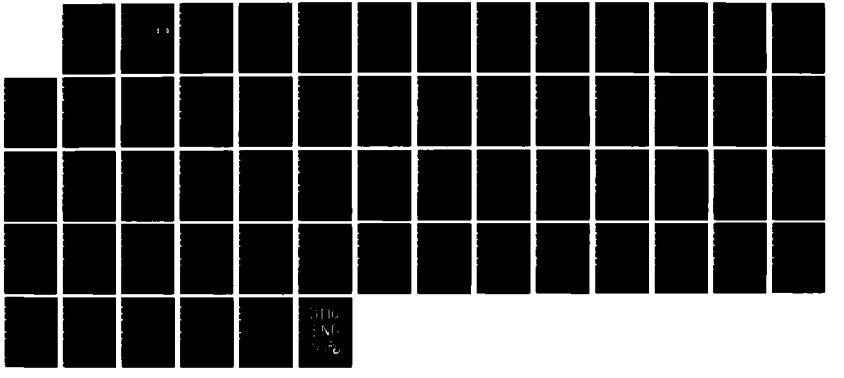

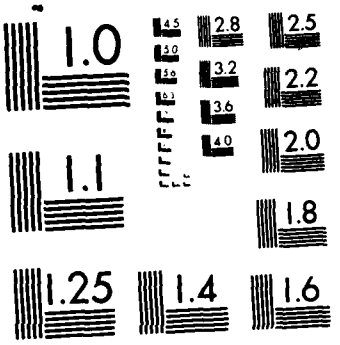

12

AFGL-TR-85-0237

# THE NEUTRAL/ION CHEMISTRY OF SODIUM IN THE STRATOSPHERE AND MESOSPHERE

José M. Rodriguez
Malcolm K. W. Ko
Nien Dak Sze

Atmospheric and Environmental Research, Inc.
840 Memorial Drive
Cambridge, Massachusetts 02139



Scientific Report No. 2

30 September 1985



AIR FORCE GEOPHYSICS LABORATORY
AIR FORCE SYSTEMS COMMAND
UNITED STATES AIR FORCE
HANSCOM AIR FORCE BASE, MASSACHUSETTS 01731

This technical report has been reviewed and is approved for publication.

WILLIAM SWIDER
Contract Manager

JOHN E. RASMUSSEN, Chief
Ionospheric Interactions Branch

FOR THE COMMANDER

ROBERT A. SKRIVANEK, Director
Ionospheric Physics Division

This report has been reviewed by the ESD Public Affairs Office (PA) and is releasable to the National Technical Information Service (NTIS).

Qualified requestors may obtain additional copies from the Defense Technical Information Center. All others should apply to the National Technical Information Service.

If your address has changed, or if you wish to be removed from the mailing list, or if the addressee is no longer employed by your organization, please notify AFGL/DAA, Hanscom AFB, MA 01731. This will assist us in maintaining a current mailing list.

SECURITY CLASSIFICATION OF THIS PAGE (When Data Entered)

| REPORT DOCUMENTATION PAGE | | READ INSTRUCTIONS BEFORE COMPLETING FORM |
|---|---|---|
| 1. REPORT NUMBER<br>AFGL-TR-85-0237 | 2. GOVT ACCESSION NO.<br>AD-A164 636 | 3. RECIPIENT'S CATALOG NUMBER |
| 4. TITLE (and Subtitle)<br>The Neutral/Ion Chemistry of Sodium in the Stratosphere and Mesosphere | | 5. TYPE OF REPORT & PERIOD COVERED<br>Scientific Report No. 2<br>6. PERFORMING ORG. REPORT NUMBER |
| 7. AUTHOR(s)<br>Jose M. Rodriguez<br>Malcolm K. W. Ko<br>Nien Dak Sze | | 8. CONTRACT OR GRANT NUMBER(s)<br>F19628-83-C-0123 |
| 9. PERFORMING ORGANIZATION NAME AND ADDRESS<br>Atmospheric and Environmental Research, Inc.<br>840 Memorial Drive<br>Cambridge, MA 02139 | | 10. PROGRAM ELEMENT, PROJECT, TASK AREA & WORK UNIT NUMBERS<br>61102F<br>2310G3BA |
| 11. CONTROLLING OFFICE NAME AND ADDRESS<br>Air Force Geophysics Laboratory<br>Hanscom AFB, MA 01731<br>Monitor: William Swider/LID | | 12. REPORT DATE<br>September 30, 1985<br>13. NUMBER OF PAGES<br>60 |
| 14. MONITORING AGENCY NAME & ADDRESS(if different from Controlling Office) | | 15. SECURITY CLASS. (of this report)<br>Unclassified<br>15a. DECLASSIFICATION/DOWNGRADING SCHEDULE |

16. DISTRIBUTION STATEMENT (of this Report)

Approved for public release;
Distribution unlimited.

17. DISTRIBUTION STATEMENT (of the abstract entered in Block 20, if different from Report)

18. SUPPLEMENTARY NOTES

19. KEY WORDS (Continue on reverse side if necessary and identify by block number)

Sodium, ion chemistry, upper atmosphere, mesosphere, photochemistry

20. ABSTRACT (Continue on reverse side if necessary and identify by block number)

This report summarizes the major finding of our research in the past contract year. Part A of the report presents results from our model calculation of the diurnal behavior of the neutral and ionic sodium species. It is shown that the concentration of $Na^+$ above 90 km exerts a direct influence on the topside scale height of the atomic sodium layer in the mesosphere. The abundance of $Na^+$ is controlled by the reaction rate for the
(continued on reverse side)

DD FORM 1 JAN 73 1473 EDITION OF 1 NOV 65 IS OBSOLETE

Unclassified
SECURITY CLASSIFICATION OF THIS PAGE (When Data Entered)

clustering reaction which is the rate limiting step for the conversion of $Na^+$ to Na. Downward transport of $Na^+$ due to ion drift is also effective in reducing the sodium abundance around 90 km. The model can successfully simulate the observed topside scale height of the sodium layer by either using a slow rate for the clustering reaction or incorporating transport of $Na^+$.

Part B of the report assesses the possible impact of sodium species on the stratospheric chlorine cycle. Recent measurements of kinetic rates suggest that the bulk of the sodium species could be in the form of NaCl in the stratosphere. Since the sodium abundance is three orders of magnitude smaller than that of chlorine, NaCl is not likely to be an important chlorine reservoir. Photolysis of NaCl could provide a mechanism for recycling HCl to Cl in the lower stratosphere if it is as fast as $10^{-3}$ $s^{-1}$. However, the mechanism would not be effective if there exists another more stable form of sodium compound, such as $NaHCO_3$ or polymers of NaCl.

TABLE OF CONTENTS

PART A

Effect of Ion Chemistry on the

Distribution of Atomic Sodium in the Mesosphere.

## 1. INTRODUCTION

In our previous report (Rodriguez et al., 1984), we presented results from our diurnal simulation of the concentrations of the sodium species based on neutral chemistry. In this report, we extend the discussion to include ion chemistry of sodium species.

Positively charged ions of atomic weight 23 have been observed in the E region during several rocket flights (see Swider, 1984, and references therein). These observations have been interpreted as positively-charged Na ion ($Na^+$). Sodium ions are produced by photo-ionization as well as by charge exchange reactions with the major positive ions $O_2^+$ and $NO^+$ (Swider, 1969a). Dissociative recombination of molecular ions produced by clustering of $Na^+$ with $N_2$ and $CO_2$ (Richter and Sechrist, 1979) ultimately removes $Na^+$ ions. The clustering rate decreases rapidly with altitude resulting in inefficient removal of ions at high altitudes. Although there are insufficient data to obtain any detailed information on the diurnal and seasonal behavior of the ions, they can nonetheless affect the behaviour of the neutral sodium. In particular, the departure of the observed scale height of atomic sodium from the scale height of the atmosphere above 90 km (Gibson and Sanford, 1970; Simonich et al., 1979) is thought to be controlled by the amount of $Na^+$ ions present (Hanson and Donaldson, 1967).

In order to calculate the production and removal rates of the sodium ions, one needs to know the distributions of the background ions. In Sections 2 and 3, we will present the model for calculating the diurnal behavior of the background ions in the D and lower E region. Section 4 will present the results of the calculated diurnal behavior of the sodium ions. The effects of the ions on the observations of the scale height of atomic sodium above 90 km and other impact on sodium will be discussed in Section 5.

## 2. IONS IN THE D AND LOWER E REGIONS

Since our primary interest is in the effect of metal ions' chemistry on the neutral chemistry around 90 km, we will use a version of the ion chemistry appropriate for the D and lower E regions. In the lower E region, production of $O_2^+$, $N_2^+$ and $O^+$ by x-ray and Lyman-β dominates. However, the $N_2^+$ and $O^+$ are converted rapidly to $O_2^+$ by charge exchange. Some $O^+$ is converted to $NO^+$, which is also formed by the charge exchange reaction of NO with $O_2^+$. In the D region, production of $NO^+$ by Lyman-α is important, making this ion the most important ionic constituent near 80 km. In the lower D region (60-80 km), there are evidence from mass-spectrometric measurements that hydrated cluster ions are common (Narcisi and Bailey, 1965; Goldberg and Aikin, 1971; Krankowsky et al., 1972). Swider and Narcisi (1983) suggested that carbon dioxide may be an important agent in hastening the formation of these clustered ions.

Negative ions are produced through a chain of reactions initiated by electron attachment to $O_2$:

$$e + O_2 + M \rightarrow O_2^- + M. \qquad (2\text{-}1)$$

Although observations show conflicting results making the identifications of the ions difficult, it is relatively certain that the major ions are $CO_3^-$ and $NO_3^-$ (Swider and Narcisi, 1983). For the problem at hand, it is not crucial that the identity of the negative ions is precisely known.

Positive ions are destroyed mainly by dissociative recombination,

$$AB^+ + e \rightarrow A + B, \qquad (2\text{-}2)$$

where $AB^+$ denotes a molecular ion. Rates for dissociative recombination are usually very fast ($\sim 10^{-6}$ cm$^3$ sec$^{-1}$), and result in lifetimes of the order of minutes for positive molecular ions near 90 km. Removal of negative ions is effected by photodetachment reactions

$$B^- + h\nu \rightarrow B + e. \qquad (2\text{-}3)$$

As the concentrations of the negative ions become much higher below 80 km at night, positive-negative ion recombination

$$A^+ + B^- \rightarrow \text{products} \qquad (2\text{-}4)$$

becomes an important loss mechanism.

A simplified model of the reaction schemes for positive and negative ions appropriate for the D and lower E region are given in Figures 1 and 2 respectively. The photo-ionization sources incorporated in our model include the following:

For daytime condition:

a)† X-rays: Absorption and ionization cross sections of O, $O_2$, and $N_2$ are taken from Swider (1969b), for wavelengths between 1 and 100Å. The solar fluxes for quiet conditions are also from Swider (1969b).

b,c) Lyman-β ionization of $O_2$ and Lyman-α ionization of NO: Absorption cross sections, ionization cross sections, and fluxes are taken from Swider (1969a, 1983) for quiet conditions.

d) Energetic electrons: Spectra of energetic electrons at 300 km measured by the AE-C satellite have been presented by Torr et al.

†Alphabet refers to labels on Figure 3.

(1976). These authors estimated an ion production rate of 10 $cm^{-3}$ $s^{-1}$ at for nighttime 90 km although the rate for daytime could be considerably higher. We have assumed that the ion production profile has the shape of the theoretical calculation of Berger et al. (1974; Figure 6, for 5 kev e-folding energy); this profile is normalized to a peak production rate of 10 $cm^{-3}$ $s^{-1}$ at 90 km. The above total production rate was subdivided into 90% $O_2^+$ and 10% $NO^+$ production as suggested by Swider (1969a, 1983) for cosmic rays. Because of the large uncertainties, production of ions from energetic electrons is not included in most of our calculations. However, they are included in Figure 3 for completeness.

e) Ionization of $O_2$ ($^1\Delta$): We have used the parameterization suggested by Paulsen et al. (1972).

f) Cosmic rays: The parameterization given by Swider (1983) for mid-latitude condition is used.

For night time conditions:

b,c) Lyman-β and Lyman-α scattered by the geocorona: The scattered fluxes as a function of altitude and solar zenith angle are taken from Strobel et al. (1974, 1980).

d) Energetic electrons: see discussion for dayside ion condition.

f) Cosmic rays: As on the dayside.

A constant production rate of $10^{-3}$ $cm^{-3}$ $s^{-1}$ at all altitudes due to galactic x-rays (Torkar and Friedrich, 1983) is included. The production of ions by starlight (Strobel et al., 1974, 1980) has been ignored since it is only important above ~ 110 km.

The adopted production rates for ions are presented for noon in Figures 3(a) and 3(b) and 3(c) for midnight. These calculations assume 45° latitude, equinox conditions. Ionization by x-rays and Lyman-β are dominant above an altitude of 90 km on the dayside. The nightside sources are dominated by ionization by energetic electrons if values from Torr et al. (1976) are adopted. We must note, however, that this source is quite variable (Torr et al., 1976). The profiles for ion production by energetic electrons presented in Figure 3 should thus be considered as upper bounds. Values for this production rates smaller than ionization by Lyman-α and Lyman-β cannot be ruled out. Uncertainties also exist in the production by Lyman-α and Lyman-β at night, since the fluxes at these wavelengths are obtained from extrapolation of radiative transfer calculations (Strobel et al., 1974, 1980).

The list of two- and three-body reactions included in the model is given in Table 1. The values for the reaction rates are taken from Swider and Narcisi (1983). Note that we have assumed that the production of $O_2^+$ ions is due only to photo-ionization processes. The additional production from charge exchange with $N_2^+$ and $O^+$ is incorporated into the same term (Swider, 1969a). The production of $NO^+$ is from both photo-ionization and charge exchange.

## 3. MODEL FOR THE BACKGROUND IONS

The basic structure of our ion code is illustrated by the flow chart in Figure 4. This code was adapted from our mesopheric code described in previous reports (see, e.g., Rodriguez et al., 1984). The local concentrations of the electron, the positive and the negative ions, are governed by the system of equations:

$$\frac{d[N_i]}{dt} = P_i - L_i[N_i] \qquad (3\text{-}1)$$

$$[e] + [NSUM] = [PSUM] \tag{3-2}$$

where $P_i$, $L_i$, and $[N_i]$ are the local production rate, loss frequency, and number density of the $i^{th}$ ionic species, [e] is the electron density, and [NSUM] and [PSUM] are the sum of the negative and positive ions concentrations, respectively. Equation (3-1) corresponds to the local approximation of the continuity equation for each ionic species whereas (3-2) serves to determine [e] by charge conservation. The numerical scheme adopted to solve the system can be used for any arbitrary grouping of the ionic species and does not assume a chain structure for the ion chemistry.

Equation (3-1) is solved at a series of discrete time steps using the fully implicit scheme described by Sze et al. (1980). The initial values for the electron and positive ion densities at noon are taken from our steady state calculation. At other time steps, the initial values are taken to be the electron and positive ion densities calculated at the previous time step. At each time step, the equations are solved using an iteration scheme similar to the one used by Swider and Foley (1978). The values for $[e]_{j+1}$ and $[PSUM]_{j+1}$ for the $j+1^{th}$ iteration are updated via (Swider & Foley, 1978)

$$\begin{aligned} [e]_{j+1} &= \{[e]_j + [PSUM]_j/(1 + \lambda)\}/2, \\ [PSUM]_{j+1} &= \{[e]_j + [NSUM]_j + [PSUM]_j\}/2 \end{aligned} \tag{3-3}$$

with

$$\lambda = [NSUM]_j/[e]_j.$$

The process is repeated until equations (3-3) are satisfied to some specified accuracy. The solution is propagated forward using time steps of one hour during the day, two hours at night, and 30 minutes around sunrise and sunset.

After 24 hours, the solutions are tested for periodicity, and the calculation is repeated if periodicity is not achieved to within 1%. Due to the small time constants for ionic processes, our solutions usually become periodic in one to two diurnal cycles.

The neutral background atmosphere is obtained from the diurnal calculation described in previous reports (see, e.g., Rodriguez et al., 1984). The effect of the ion chemistry on neutral background trace gases is negligible under most conditions.

Results of our calculations for the background ions and electrons at 45°N for equinox condition are presented below. The diurnal variation of the electron density is presented in Figure 5 at altitudes of 86, 90, 94, and 100 km. Similar results for the same altitudes are shown in Figure 6 for $O_2^+$ and $NO^+$, which are the main positive ion constituents in this region. The electron densities exhibit a day-to-night ratio of about 20 - 30 between 86 and 94 km, increasing to about 50 at 100 km. There is considerable variation during the daytime, with the electron density increasing by factors of 2 to 5 between sunrise and noon. $NO^+$ densities are larger than $O_2^+$ densities over most of this region; the diurnal behavior of $NO^+$ is thus positively correlated with that of the electrons. Below 95 km, $O_2^+$ densities exhibit a larger day-to-night ratio (greater than 200). This is due to the conversion of $O_2^+$ to $NO^+$ at night through charge exchange with NO.

Our results during the day are in good agreement with diurnal calculations presented by Torkar and Friedrich (1983). We note that the magnitude of the diurnal variation, however, will depend on the model's assumptions for nightside sources. The ionization by energetic electrons exhibits great variability. In these calculations, we neglect ion production by energetic electrons. The Lyman-$\alpha$ and Lyman-$\beta$ sources are computed from radiative transfer

models which become uncertain below ~ 100 km (Strobel et al., 1974, 1980). Our results should be interpreted only as the general diurnal behavior of electrons and ions. More detailed information on the nightside ionization sources at specific times is needed to pinpoint the diurnal variation to a greater accuracy.

Profiles for electron and total negative ion densities for day and night are shown in Figure 7 for the same conditions as in Figures 5 and 6. In light of the possibly large variability in the electron flux, we also include the calculated profiles for which the ionization from energetic electrons at night is included (curves e, f). The figure illustrates that variability of this source can induce changes in the electron density of more than factors of 4 above 90 km.

The distributions of negative ions for daytime and nighttime conditions are given in Figure 8. The total negative ion density in the daytime remains smaller than the electron density down to about 60 km. During the night, the concentration of the negative ions becomes larger in the absence of photodetachment reaction (2-4). The density of $NO_3^-$ grows to more than $10^3$ $cm^{-3}$, reflecting the increase in concentrations of $NO_2$ and $O_3$ which favors the transfer to $NO_3^-$ via $O_3^-$ and $CO_3^-$. Hydrated negative ions are not included in the calculation since the rates for the reactions involving these ions are uncertain.

Profiles of positive ions for day- and nighttime conditions are given in Figures 9 and 10. The positive ions are mostly in the form of $O_2^+$ and $NO^+$ above 90 km. Below 90 km, various hydrated ions are formed in appreciable amounts. Densities for these ions are shown in Figure 10. Formation of these hydrated ions is initiated by the clustering reactions (Swider and Narcisi, 1983):

$$H_3O^+ + N_2 - M \rightarrow H_3O^+ \cdot N_2 + M,$$
$$NO^+ + N_2 + N_2 \rightarrow NO^+ \cdot N_2 + N_2, \quad (3\text{-}4)$$
$$NO^+ + CO_2 + N_2 \rightarrow NO^+ \cdot CO_2 + N_2,$$

followed by switching reactions of the form

$$A^+ \cdot N_2 + CO_2 \rightarrow A^+ \cdot CO_2 + N_2, \quad (3\text{-}5)$$
$$A^+ \cdot CO_2 + H_2O \rightarrow A^+ \cdot H_2O + CO_2.$$

The profiles in Figures 9 and 10 are calculated using the $H_2O$ mixing ratios of Bevilarqua et al. (1983), which are up to an order of magnitude smaller than those of Allen et al. (1984) above 80 km. Variations in upper mesospheric water will affect the calculated densities of the hydrated positive ions. The results in Figures 9 and 10 reproduce the general characteristics of calculations by other models (Swider and Foley, 1978; Swider, 1983; Swider and Narcisi, 1983).

## 4. DIURNAL MODEL FOR SODIUM NEUTRALS AND IONS

The ionic sodium species considered are: $Na^+$, $NaO^+$, $NaO_2^+$, $Na^+ \cdot N_2$, $Na^+ \cdot CO_2$, and $Na^+ \cdot H_2O$. The chemical scheme for this family is illustrated in Figure 11. This scheme combines the reactions proposed by Murad (1978) and Richter and Sechrist (1979). The latter paper proposed the clustering scheme that recycles the $Na^+$ back to neutral Na.

The $Na^+$ ion is produced by

$$Na + h\nu \rightarrow Na^+ + e, \quad (4\text{-}1)$$
$$Na + O_2^+ \rightarrow Na^+ + O_2, \quad (4\text{-}2)$$

and

$$Na + NO^+ \rightarrow Na^+ + NO. \quad (4\text{-}3)$$

Molecular ions are formed via

$$Na^+ + N_2 + M \rightarrow Na^+ \cdot N_2 + M \qquad (4\text{-}4)$$

which in turn yields the more stable $Na^+ \cdot CO_2$ and $Na^+ \cdot H_2O$ through the switching reactions:

$$Na^+ \cdot N_2 + CO_2 \rightarrow Na^+ \cdot CO_2 + N_2 \qquad (4\text{-}5)$$

and

$$Na^+ \cdot CO_2 + H_2O \rightarrow Na^+ \cdot H_2O + CO_2 \cdot \qquad (4\text{-}6)$$

The cluster ions are converted back to neutral atomic sodium by dissociative recombination. Reaction (4-4) is the rate limiting step for the sequence of reactions (4-4) through (4-6).

The ion reactions shown in Figure 11 are added to our diurnal model for the sodium species (Rodriguez et al., 1984), and the diurnal behavior and altitude distributions of the ionic and neutral sodium species are calculated in a self-consistent manner. In these calculations, the background neutral and ionic constituents are not recalculated, since they are not affected by the sodium chemistry. Parameters used in calculating the reaction rates in our sodium model are shown in Table 2, with the rates for the neutral species as documented in Rodriguez et al. (1984) and those for the ionic species taken from Murad (1978) and Richter and Sechrist (1979). As in the case of the neutral chemistry, most of the ion reactions have not been measured, and the values proposed are deduced from measured values of similar reactions.

The diurnal variation of $Na^+$ is shown in Figure 12 for 90, 94, and 100 km. The day-to-night ratio ranges from 400 (90 km) to 3 (100 km). The factor of 10 variation for the altitude range 90 to 110 km suggested by the data as presented by Swider (1984) is thus consistent with our results, although the large changes in diurnal variation over a small altitude range preclude drawing any definitive conclusions about the validity of our chemical scheme.

Altitude profiles at noon for $Na^+$ and Na are shown in Figure 13. Atomic sodium is converted into $Na^+$ at high altitudes where their densities are comparable. As we shall see in the next section, processes that affect the concentration of $Na^+$ can then indirectly alter the distributions of Na at these altitudes. Densities of the other ionic species are smaller by factors of 100 or more. In particular, the $[NaO^+]/[Na^+]$ value is $\sim 10^{-7}$ to $10^{-8}$, in agreement with the estimations of Murad (1978).

## 5. SODIUM ION CHEMISTRY AND THE SCALE HEIGHT OF THE NEUTRAL ATOMIC SODIUM LAYER

The topside scale height of the sodium layer has been observed to be much smaller than that of the background atmosphere (Gibson and Sandford, 1971; Megie and Blamont, 1977; Simonich et al., 1979; Granier and Megie, 1982), decreasing to about 2-4 km at 100 km altitude. A possible explanation for this small scale height is the conversion of Na to $Na^+$ by photoionization or charge exchange with $O_2^+$ (Hanson and Donaldson, 1967; Gadsden, 1968; Richter and Sechrist, 1979).

This sensitivity of the scale height of atomic Na ion chemistry is illustrated in Figure 14 which gives the calculated profiles of Na with different assumptions for the $Na^+$ abundance. As discussed in Section 4, reaction (4-4) constitutes the rate-limiting step for recombination of sodium ions and is assumed to be of the form (Richter and Sechrist, 1979):

$$K_S = K^* \left(\frac{300}{T}\right)^{1.5} \text{ cm}^6 \text{ s}^{-1}. \qquad (5\text{-}1)$$

A value of $K^* = 2 \times 10^{-31}$ cm$^6$ s$^{-1}$ was suggested by Richter and Sechrist (1979) by analogy to similar reactions involving $NO^+$. Reaction (4-4) has also been measured at 130° K in a helium buffer by Perry et al. (1980); their value of $2.6 \times 10^{-30}$ cm$^6$ s$^{-1}$ implies a value of $K^* = 7 \times 10^{-31}$ cm$^6$ s$^{-1}$ if the temperature dependence in eq. (5-1) is valid. The Na profiles in Figure 14 are calculated using different values for K*. The noontime profile from the calculation without ionic species (-o-) is compared with the cases calculated with value of K* from Richter and Sechrist (1979) ($K^* = 2 \times 10^{-31}$ cm$^6$ s$^{-1}$, ___) and Perry et al. (1980) ($K^* = 7 \times 10^{-31}$ cm$^6$ s$^{-1}$, ---). We have also considered the hypothetical situation with $K^* = 4 \times 10^{-32}$ cm$^6$ s$^{-1}$ (~~XXX~~). As expected, the scale height of neutral sodium increases with increasing K*, reflecting the more efficient rate for reconversion of $Na^+$ to Na. The observed small scale heights about 90 km could thus be explained by the ion chemistry without having to invoke transport processes (as in Hanson and Donaldson, 1967, for example) if $K_S$ is sufficiently fast.

Local values for the topside scale height are given in Table 3 for the cases considered in Figure 14. A comparison with observations indicates an upper limit of $2 \times 10^{-31}$ cm$^6$ s$^{-1}$ for K* if the small topside scale heights are to be explained solely by ion-neutral chemistry. Such small values of K* are not likely, however, given the measurements of Perry et al. (1980) and that the faster clustering rate are expected when $N_2$ is the buffer gas (Jegou et al., 1984; Heimerl, 1976). An alternative mechanism to reduce the topside scale height is the downward transport of $Na^+$ from the region prior to its conversion to Na. Vertical ion drifts with velocities of 10 to 50 cm s$^{-1}$ have been suggested by Hunten (1981) and Kirchoff and Batista (1984) and could be effective.

Ionic species could acquire a vertical velocity through electromagnetic interactions. These include electrostatic forces from the ionospheric electric fields (Kirchoff and Batista, 1984) and $\bar{v} \times \bar{B}$ type forces from the magnetic field because of the motions in the horizontal plane associated with the zonal wind (Jegou et al., 1984) and tides (Kirchoff and Batista, 1984). Ion drift could provide an effective way for the vertical transport of Na species in the mesosphere, particularly when a significant portion of the sodium species is in ionic form.

A detailed calculation of these effects would require the incorporation of the above parameters in our model. In lieu of a full calculation, we examined the response of the topside layer to typical net vertical downward velocities for ions by modifying the continuity equation for the NaX species to ha.. the form

$$\frac{d\phi}{dz} + \frac{d[([Na^+]/[NaX]) \cdot [NaX] \cdot W_D]}{dz} = P - L, \qquad (5\text{-}2)$$

where $\phi$ is the flux due to molecular and eddy diffusion, P and L denote the production and loss mechanisms for NaX, and $W_D$ represents the vertical ion drift velocity. The relative abundance $[Na^+]/[NaX]$ is independent of the assumed drift velocity if the time constant for the vertical drift is larger than the time constant for the removal of $Na^+$ as given by the rate limiting step (4-4). This condition is valid below 100 km, where the time constant for the vertical drift is $\sim 10^4$ s, while the time constant for $Na^+$ clustering is $\sim 10^3$ s.

Figure 15 shows the results of our calculations for constant drift velocities equal to 0, -5, -10, and -20 cm/s between 120 and 90 km. The small topside scale height observed (2-3 km, Gibson and Sandford, 1981; Clemesha et

al., 1982) can be modeled using downward velocities between 10 and 20 cm/s. The effect of vertical ion drift is thus an important contributing factor in controlling the topside sodium layer.

## 6. CONCLUDING REMARKS

We have presented the results of a fully diurnal model for ion species in the D and lower E regions. When coupled with our previous model of the neutral species, our present model allows for the self-consistent calculation of background neutral and ionic species between 60 and 120 km. Results of our calculations are in good agreement with those of other models.

Production of $Na^+$ occurs primarily through photoionization below 100 km, and through charge exchange with $O_2^+$ at higher altitudes. The main loss mechanism is dissociative recombination of sodium cluster ions. A self-consistent calculation thus requires knowledge of the $O_2^+$ and e densities in the above altitude regimes. Our code has been applied to the calculation of the density and diurnal variation of sodium species above 90 km. The calculated diurnal variation of $Na^+$ (factor of 10-100 between 90 and 100 km) and daytime densities ($\sim 10^2$ $cm^{-3}$) are in good agreement with rocket data (Swider, 1984).

We have also investigated the effect of ion chemistry on the abundance of neutral sodium above 90 km. In particular, the small scale height (2-3 km) observed in the topside sodium layer seems to require either downward ion drifts velocities of order 10-20 cm $s^{-1}$ above 90 km or a rate of clustering of $Na^+$ with $N_2$ a factor of 5 smaller than the value suggested by Richter and Sechrist (1979). Further elucidation of this question will require measurements of the clustering rate at mesospheric temperatures as well as incorporation of more realistic scenarios for ion drifts into our model.

Since we have included a complete treatment of the ion chemistry in the D region, the model presented above is also suited to studies of the D region ion chemistry and its possible effect on neutral constituents during disturbed conditions (Swider and Keneshea, 1973; Solomon et al., 1983). The model also allows for each extension to the calculation of other metallic ion species.

Table 1

**List of Reactions and Reaction Rates for the Background Ions**

| | TYPE[a] | PAR1 | PAR2 | PAR3 | REACTIONS |
|---|---|---|---|---|---|
| 1 | 7. | 1.00E-28 | -3.00E+00 | 0.00E+00 | $H^+.(H_2O)_3 + CO_2 + M = H^+.(H_2O)_3.CO_2 + M$, 7 |
| 2 | 1. | 1.00E-09 | 0.00E+00 | 0.00E+00 | $H^+.(H_2O)_3.CO_2 + H_2O = H^+.(H_2O)_4 + CO_2$, 1 |
| 3 | 1. | 4.50E-10 | 0.00E+00 | 0.00E+00 | $O_2^+ + NO = NO^+ + O_2$, 1 |
| 4 | 7. | 1.60E-30 | -3.20E+00 | 0.00E+00 | $O_2^+ + O_2 + M = O_4^+ + M$, 7 |
| 5 | 1. | 3.00E-10 | 0.00E+00 | 0.00E+00 | $O_4^+ + O = O_2^+ + O_3$, 1 |
| 6 | 1. | 1.50E-09 | 0.00E+00 | 0.00E+00 | $O_4^+ + H_2O = O_2^+.H_2O + O_2$, 1 |
| 7 | 1. | 1.00E-09 | 0.00E+00 | 0.00E+00 | $O_2^+.H_2O + H_2O = H^+.H_2OOH + O_2$, 1 |
| 8 | 1. | 2.00E-10 | 0.00E+00 | 0.00E+00 | $O_2^+.H_2O + H_2O = H^+.H_2O + OH$, 1 |
| 9 | 1. | 1.40E-09 | 0.00E+00 | 0.00E+00 | $H^+.H_2OOH + H_2O = H^+.(H_2O)_2 + OH$, 1 |
| 10 | 7. | 1.40E-30 | -2.00E+00 | 0.00E+00 | $H^+.H_2O + N_2 + N_2 = H^+.H_2O.N_2 + N_2$, 7 |
| 11 | 1. | 1.00E-09 | 0.00E+00 | 0.00E+00 | $H^+.H_2O.N_2 + CO_2 = H^+.H_2O.CO_2 + N_2$, 1 |
| 12 | 1. | 1.00E-09 | 0.00E+00 | 0.00E+00 | $H^+.H_2O.CO_2 + H_2O = H^+.(H_2O)_2 + CO_2$, 1 |
| 13 | 7. | 5.00E-28 | -3.00E+00 | 0.00E+00 | $H^+.(H_2O)_2 + CO_2 + M = H^+.(H_2O)_2CO_2 + M$, 7 |
| 14 | 1. | 1.00E-09 | 0.00E+00 | 0.00E+00 | $H^+.(H_2O)_2CO_2 + H_2O = H^+.(H_2O)_3 + CO_2$, 1 |
| 15 | 7. | 3.50E-27 | -3.00E+00 | 0.00E+00 | $H^+.H_2O + H_2O + M = H^+.(H_2O)_2 + M$, 7 |
| 16 | 7. | 2.20E-27 | -3.00E+00 | 0.00E+00 | $H^+.(H_2O)_2 + H_2O + M = H^+.(H_2O)_3 + M$, 7 |
| 17 | 7. | 2.30E-27 | -3.00E+00 | 0.00E+00 | $H^+.(H_2O)_3 + H_2O + M = H^+.(H_2O)_4 + M$, 7 |
| 18 | 7. | 1.00E-29 | -2.30E+00 | 0.00E+00 | $NO^+ + CO_2 + N_2 = NO^+.CO_2 + N_2$, 7 |
| 19 | 1. | 1.00E-09 | 0.00E+00 | 0.00E+00 | $NO^+.CO_2 + H_2O = CO_2 + NO^+.H_2O$, 1 |
| 20 | 7. | 1.10E-27 | -4.70E+00 | 0.00E+00 | $NO^+.H_2O + H_2O + N_2 = NO^+.(H_2O)_2 + N_2$, 7 |
| 21 | 7. | 1.60E-27 | -4.70E+00 | 0.00E+00 | $NO^+.(H_2O)_2 + H_2O + N_2 = NO^+.(H_2O)_3 + N_2$, 7 |
| 22 | 1. | 7.00E-11 | 0.00E+00 | 0.00E+00 | $NO^+.(H_2O)_3 + H_2O = H^+.(H_2O)_3 + XX$, 1 |
| 23 | 7. | 4.00E-07 | -1.00E+00 | 0.00E+00 | $NO^+ + E = N + O$, 7 |
| 24 | 7. | 2.10E-07 | -6.30E-01 | 0.00E+00 | $O_2^+ + E = O + O$, 7 |
| 25 | 1. | 2.00E-06 | 0.00E+00 | 0.00E+00 | $O_4^+ + E = O_2 + O_2$, 1 |
| 26 | 1. | 1.50E-06 | 0.00E+00 | 0.00E+00 | $O_2^+.H_2O + E = O_2 + H_2O$, 1 |

[a]The parameterization and values for the reaction constants are taken from Swider and Narcisi (1984). The reaction rates are calculated as follows:

Type 1: $k = PAR1$

Type 7: $k = PAR1*(300/T)^{-PAR2}$

Type 8: $k = PAR1*(300/T)^{-PAR2}*\exp(PAR3/T)$.

| | TYPE | PAR1 | PAR2 | PAR3 | REACTIONS |
|---|---|---|---|---|---|
| 27 | 1. | 2.00E-06 | 0.00E+00 | 0.00E+00 | $H^+.H_2OOH + E = H_2O + H_2O$, 1 |
| 28 | 1. | 1.30E-06 | 0.00E+00 | 0.00E+00 | $H^+.H_2O + E = H_2 + OH$, 1 |
| 29 | 1. | 2.50E-06 | 0.00E+00 | 0.00E+00 | $H^+.(H_2O)_2 + E = H_2O + H_2 + OH$, 1 |
| 30 | 1. | 3.00E-06 | 0.00E+00 | 0.00E+00 | $H^+.(H_2O)_3 + E = OH + XX$, 1 |
| 31 | 1. | 3.60E-06 | 0.00E+00 | 0.00E+00 | $H^+.(H_2O)_4 + E = OH + XX$, 1 |
| 32 | 1. | 1.50E-06 | 0.00E+00 | 0.00E+00 | $H^+.H_2O.N_2 + E = H + XX$, 1 |
| 33 | 1. | 2.00E-06 | 0.00E+00 | 0.00E+00 | $H^+.H_2O.CO_2 + E = H + XX$, 1 |
| 34 | 1. | 3.00E-06 | 0.00E+00 | 0.00E+00 | $H^+.(H_2O)_2CO_2 + E = H + XX$, 1 |
| 35 | 1. | 1.50E-06 | 0.00E+00 | 0.00E+00 | $NO^+.CO_2 + E = NO + CO_2$, 1 |
| 36 | 1. | 1.50E-06 | 0.00E+00 | 0.00E+00 | $NO^+.H_2O + E = NO + H_2O$, 1 |
| 37 | 1. | 2.00E-06 | 0.00E+00 | 0.00E+00 | $NO^+.(H_2O)_2 + E = NO + XX$, 1 |
| 38 | 1. | 3.00E-06 | 0.00E+00 | 0.00E+00 | $NO^+.(H_2O)_3 + E = NO + XX$, 1 |
| 39 | 8. | 3.30E-06 | -4.00E+00 | -5.03E+03 | $O_4^+ + M = O_2^+ + O_2 + M$, 8 |
| 40 | 7. | 2.00E-31 | -4.40E+00 | 0.00E+00 | $NO^+ + N_2 + N_2 = NO^+.N_2 + N_2$, 7 |
| 41 | 1. | 1.00E-09 | 0.00E+00 | 0.00E+00 | $NO^+.N_2 + CO_2 = NO^+.CO_2 + N_2$, 1 |
| 42 | 8. | 1.00E-08 | -5.40E+00 | -2.10E+03 | $NO^+.N_2 + N_2 = NO^+ + N_2 + N_2$, 8 |
| 43 | 7. | 2.00E-31 | -4.40E+00 | 0.00E+00 | $NO^+.H_2O + N_2 + N_2 = NO^+.H_2O.N_2 + N_2$, 7 |
| 44 | 1. | 1.00E-09 | 0.00E+00 | 0.00E+00 | $NO^+.H_2O.N_2 + CO_2 = NO^+.H_2OCO_2 + N_2$, 1 |
| 45 | 1. | 1.00E-09 | 0.00E+00 | 0.00E+00 | $NO^+.H_2O.CO_2 + H_2O = NO^+.(H_2O)_2 + CO_2$, 1 |
| 46 | 7. | 2.00E-31 | -4.40E+00 | 0.00E+00 | $NO^+.(H_2O)_2 + N_2 + N_2 = NO^+.(H_2O)_2.N_2 + N_2$, 7 |
| 47 | 1. | 1.00E-09 | 0.00E+00 | 0.00E+00 | $NO^+.(H_2O)_2.N_2 + CO_2 = NO^+.(H_2O)_2.CO_2 + N_2$, 1 |
| 48 | 1. | 1.00E-09 | 0.00E+00 | 0.00E+00 | $NO^+.(H_2O)_2.CO_2 + H_2O = NO^+.(H_2O)_3 + CO_2$, 1 |
| 49 | 8. | 1.20E-01 | -4.00E+00 | -8.80E+03 | $H^+.(H_2O)_4 + M = H^+.(H_2O)_3 + H_2O + M$, 8 |
| 50 | 8. | 2.00E-05 | -3.30E+00 | -5.50E+03 | $NO^+.CO_2 + M = NO^+ + CO_2 + M$, 8 |
| 51 | 8. | 5.00E-08 | -5.40E+00 | -2.10E+03 | $NO^+.H_2O.N_2 + M = NO^+.H_2O + N_2 + M$, 8 |
| 52 | 8. | 2.00E-04 | -3.30E+00 | -5.50E+03 | $NO^+.H_2O.CO_2 + M = NO^+.H_2O + CO_2 + M$, 8 |
| 53 | 8. | 5.00E-07 | -5.40E+00 | -2.10E+03 | $NO^+.(H_2O)_2.N_2 + M = NO^+.(H_2O)_2 + N_2 + M$, 8 |
| 54 | 8. | 2.00E-03 | -3.30E+00 | -5.50E+03 | $NO^+.(H_2O)_2.CO_2 + M = NO^+.(H_2O)_2 + CO_2 + M$, 8 |
| 55 | 8. | 1.00E-02 | -5.70E+00 | -6.80E+03 | $NO^+.(H_2O)_3 + M = NO^+.(H_2O)_2 + H_2O + M$, 8 |
| 56 | 8. | 1.00E-02 | -5.70E+00 | -8.10E+03 | $NO^+.(H_2O)_2 + M = NO^+.H_2O + H_2O + M$, 8 |
| 57 | 1. | 5.00E-10 | 0.00E+00 | 0.00E+00 | $O_2^- + O_3 = O_3^- + O_2$, 1 |
| 58 | 8. | 1.40E-29 | -1.00E+00 | -6.00E+02 | $O_2 + E + O_2 = O_2^- + O_2$, 8 |
| 59 | 1. | 1.00E-31 | 0.00E+00 | 0.00E+00 | $O_2 + E + N_2 = O_2^- + N_2$, 1 |
| 60 | 1. | 1.50E-10 | 0.00E+00 | 0.00E+00 | $O_2^- + O = O_3 + E$, 1 |

| | TYPE | PAR1 | PAR2 | PAR3 | REACTION |
|---|---|---|---|---|---|
| 61 | 1. | 1.50E-10 | 0.00E+00 | 0.00E+00 | $O_2^- + O = O^- + O_2$, 1 |
| 62 | 1. | 2.00E-10 | 0.00E+00 | 0.00E+00 | $O_2^- + O_2(^1\Delta) = O_2 + O_2 + E$, 1 |
| 63 | 7. | 2.50E-30 | -2.50E+00 | 0.00E+00 | $O_2^- + O_2 + O_2 = O_4^- + O_2$, 7 |
| 64 | 1. | 4.30E-10 | 0.00E+00 | 0.00E+00 | $O_4^- + CO_2 = CO_4^- + O_2$, 1 |
| 65 | 1. | 1.30E-10 | 0.00E+00 | 0.00E+00 | $CO_4^- + O_3 = O_3^- + CO_2 + O_2$, 1 |
| 66 | 1. | 4.80E-11 | 0.00E+00 | 0.00E+00 | $CO_4^- + NO = NO_3^- + CO_2$, 1 |
| 67 | 1. | 1.50E-10 | 0.00E+00 | 0.00E+00 | $CO_4^- + O = CO_3^- + O_2$, 1 |
| 68 | 1. | 3.20E-10 | 0.00E+00 | 0.00E+00 | $O_3^- + O = O_2^- + O_2$, 1 |
| 69 | 1. | 5.50E-10 | 0.00E+00 | 0.00E+00 | $O_3^- + CO_2 = CO_3^- + O_2$, 1 |
| 70 | 1. | 1.10E-10 | 0.00E+00 | 0.00E+00 | $CO_3^- + O = O_2^- + CO_2$, 1 |
| 71 | 1. | 1.10E-11 | 0.00E+00 | 0.00E+00 | $CO_3^- + NO = NO_2^- + CO_2$, 1 |
| 72 | 1. | 2.00E-10 | 0.00E+00 | 0.00E+00 | $CO_3^- + NO_2 = NO_3^- + CO_2$, 1 |
| 73 | 1. | 9.00E-11 | 0.00E+00 | 0.00E+00 | $NO_2^- + O_3 = NO_3^- + O_2$, 1 |
| 74 | 7. | 5.00E-30 | -1.90E+00 | 0.00E+00 | $O^- + O_2 + O_2 = O_3^- + O_2$, 7 |
| 75 | 1. | 2.00E-10 | 0.00E+00 | 0.00E+00 | $O^- + O = O_2 + E$, 1 |
| 76 | 1. | 3.00E-10 | 0.00E+00 | 0.00E+00 | $O^- + O_2(^1\Delta) = O_3 + E$, 1 |
| 77 | 1. | 4.40E-10 | 0.00E+00 | 0.00E+00 | $O^- + O_3 = O_3^- + O$, 1 |
| 78 | 1. | 4.40E-10 | 0.00E+00 | 0.00E+00 | $O^- + O_3 = O_2^- + O_2$, 1 |
| 79 | 1. | 6.00E-08 | 0.00E+00 | 0.00E+00 | $O_2^+ + [NSUM] = XX$, 1 |
| 80 | 1. | 6.00E-08 | 0.00E+00 | 0.00E+00 | $O_4^+ + [NSUM] = XX$, 1 |
| 81 | 1. | 6.00E-08 | 0.00E+00 | 0.00E+00 | $O_2 + H_2O + [NSUM] = XX$, 1 |
| 82 | 1. | 6.00E-08 | 0.00E+00 | 0.00E+00 | $H^+.H_2O.OH + [NSUM] = XX$, 1 |
| 83 | 1. | 6.00E-08 | 0.00E+00 | 0.00E+00 | $H^+.H_2O + [NSUM] = XX$, 1 |
| 84 | 1. | 6.00E-08 | 0.00E+00 | 0.00E+00 | $H^+.H_2O.N_2 + [NSUM] = XX$, 1 |
| 85 | 1. | 6.00E-08 | 0.00E+00 | 0.00E+00 | $H^+.H_2O.CO_2 + [NSUM] = XX$, 1 |
| 86 | 1. | 6.00E-08 | 0.00E+00 | 0.00E+00 | $H.(H_2O)_2^+ + [NSUM] = XX$, 1 |
| 87 | 1. | 6.00E-08 | 0.00E+00 | 0.00E+00 | $H.(H_2O)_2.CO_2 + [NSUM] = XX$, 1 |
| 88 | 1. | 6.00E-08 | 0.00E+00 | 0.00E+00 | $H^+.(H_2O)_3 + [NSUM] = XX$, 1 |
| 89 | 1. | 6.00E-08 | 0.00E+00 | 0.00E+00 | $H^+.(H_2O)_3.CO_2 + [NSUM] = XX$, 1 |
| 90 | 1. | 6.00E-08 | 0.00E+00 | 0.00E+00 | $H^+.(H_2O)_4 + [NSUM] = XX$, 1 |
| 91 | 1. | 6.00E-08 | 0.00E+00 | 0.00E+00 | $NO^+ + [NSUM] = XX$, 1 |
| 92 | 1. | 6.00E-08 | 0.00E+00 | 0.00E+00 | $NO^+.N_2 + [NSUM] = XX$, 1 |
| 93 | 1. | 6.00E-08 | 0.00E+00 | 0.00E+00 | $NO^+.CO_2 + [NSUM] = XX$, 1 |
| 94 | 1. | 6.00E-08 | 0.00E+00 | 0.00E+00 | $O_2^- + [PSUM] = XX$, 1 |

| | TYPE | PAR1 | PAR2 | PAR3 | REACTION |
|---|---|---|---|---|---|
| 95 | 1. | 6.00E-08 | 0.00E+00 | 0.00E+00 | $O^-$ + [PSUM] = XX, 1 |
| 96 | 1. | 6.00E-08 | 0.00E+00 | 0.00E+00 | $O_4^-$ + [PSUM] = XX, 1 |
| 97 | 1. | 6.00E-08 | 0.00E+00 | 0.00E+00 | $O_3^-$ + [PSUM] = XX, 1 |
| 98 | 1. | 6.00E-08 | 0.00E+00 | 0.00E+00 | $CO_3^-$ + [PSUM] = XX, 1 |
| 99 | 1. | 6.00E-08 | 0.00E+00 | 0.00E+00 | $CO_4^-$ + [PSUM] = XX, 1 |
| 100 | 1. | 6.00E-08 | 0.00E+00 | 0.00E+00 | $NO_2^-$ + [PSUM] = XX, 1 |
| 101 | 1. | 6.00E-08 | 0.00E+00 | 0.00E+00 | $NO_3^-$ + [PSUM] = XX, 1 |
| 102 | 1. | 6.00E-08 | 0.00E+00 | 0.00E+00 | $NO^+.H_2O$ + [NSUM] = XX, 1 |
| 103 | 1. | 6.00E-08 | 0.00E+00 | 0.00E+00 | $NO^+.(H_2O)_2$ + [NSUM] = XX, 1 |
| 104 | 1. | 6.00E-08 | 0.00E+00 | 0.00E+00 | $NO^+.(H_2O)_3$ + [NSUM] = XX, 1 |
| 105 | 1. | 6.00E-08 | 0.00E+00 | 0.00E+00 | $NO^+.H_2O.N_2$ + [NSUM] = XX, 1 |
| 106 | 1. | 6.00E-08 | 0.00E+00 | 0.00E+00 | $NO^+.H_2O.CO_2$ + [NSUM] = XX, 1 |
| 107 | 1. | 6.00E-08 | 0.00E+00 | 0.00E+00 | $NO^+.(H_2O)_2.N_2$ + [NSUM] = XX, 1 |
| 108 | 1. | 6.00E-08 | 0.00E+00 | 0.00E+00 | $NO^+.(H_2O)_2.CO_2$ + [NSUM] = XX, 1 |

Table 2

**List of Reactions for the Sodium Species**

| | TYPE[a] | PAR1 | PAR2 | PAR3 | REACTIONS |
|---|---|---|---|---|---|
| 1 | 1. | 3.00E-10 | 0.00E+00 | 0.00E+00 | $Na + O_3 = NaO + O_2$, 1 |
| 2 | 1. | 4.00E-11 | 0.00E+00 | 0.00E+00 | $NaO + O = Na + O_2$, 1 |
| 3 | 2. | 8.00E-31 | -2.90E+02 | 0.00E+00 | $Na^+O_2 + M = NaO_2 + M$, 2 |
| 4 | 1. | 1.00E-13 | 0.00E+00 | 0.00E+00 | $NaO_2 + O = NaO + O_2$, 1 |
| 5 | 1. | 0.00E+00 | 0.00E+00 | 0.00E+00 | $NaO + H_2O = NaOH + OH$, 1 |
| 6 | 1. | 5.00E-11 | 0.00E+00 | 0.00E+00 | $NaO + O_3 = NaO_2 + O_2$, 1 |
| 7 | 1. | 1.00E-14 | 0.00E+00 | 0.00E+00 | $NaO + H = Na + OH$, 1 |
| 8 | 1. | 1.00E-11 | 0.00E+00 | 0.00E+00 | $NaO_2 + OH = NaOH + O_2$, 1 |
| 9 | 1. | 1.00E-13 | 0.00E+00 | 0.00E+00 | $NaO_2 + H = NaOH + O$, 1 |
| 10 | 1. | 1.40E-12 | 0.00E+00 | 0.00E+00 | $NaOH + H = Na + H_2O$, 1 |
| 11 | 1. | 1.00E-10 | 0.00E+00 | 0.00E+00 | $NaOH + O^1D = NaO + OH$, 1 |
| 12 | 1. | 1.40E-11 | 0.00E+00 | 0.00E+00 | $Na + HO_2 = NaOH + O$, 1 |
| 13 | 1. | 1.00E-10 | 0.00E+00 | 0.00E+00 | $NaO + O_3 = Na + XX$, 1 |
| 14 | 1. | 1.00E-11 | 0.00E+00 | 0.00E+00 | $NaO + HO_2 = NaOH + XX$, 1 |
| 15 | 1. | 6.00E-10 | 0.00E+00 | 0.00E+00 | $Na + O_2^+ = Na^+ + O_2$, 1 |
| 16 | 1. | 8.00E-11 | 0.00E+00 | 0.00E+00 | $Na + NO^+ = Na^+ + NO$, 1 |
| 17 | 7. | 2.00E-31 | -1.50E+00 | 0.00E+00 | $Na^+ + N_2 + M = Na^+.N_2 + M$, 7 |
| 18 | 8. | 9.00E-07 | -2.50E+00 | -4.75E+03 | $Na^+.N_2 + M = Na^+ + N_2 + N_2$, 8 |
| 19 | 7. | 2.00E-29 | -1.50E+00 | 0.00E+00 | $Na^+ + CO_2 + M = Na^+.CO_2 + M$, 7 |
| 20 | 8. | 6.00E-06 | -2.50E+00 | -6.25E+03 | $Na^+.CO_2 + M = Na^+ + CO_2 + M$, 8 |
| 21 | 7. | 5.00E-32 | -1.50E+00 | 0.00E+00 | $Na^+ + O_2 + M = NaO_2^+ + M$, 7 |
| 22 | 8. | 8.00E-09 | -2.50E+00 | -2.85E+03 | $NaO_2^+ + M = Na^+ + O_2 + M$, 8 |
| 23 | 7. | 1.00E-28 | -1.50E+00 | 0.00E+00 | $Na^+ + H_2O + M = Na^+.H_2O + M$, 7 |
| 24 | 1. | 1.00E-09 | 0.00E+00 | 0.00E+00 | $Na^+.N_2 + CO_2 = Na^+.CO_2 + N_2$, 1 |
| 25 | 1. | 1.00E-09 | 0.00E+00 | 0.00E+00 | $Na^+.CO_2 + H_2O = Na^+.H_2O + CO_2$, 1 |
| 26 | 7. | 1.00E-06 | -5.00E-01 | 0.00E+00 | $Na^+.CO_2 + E = Na + CO_2$, 7 |

[a]The parameterization and values for the reaction constants are taken from Swider and Narcisi (1984). The reaction rates are calculated as follows:

Type 1: $k = PAR1$

Type 2: $k = PAR1*\exp(-PAR2/T)$

Type 7: $k = PAR1*(300/T)^{-PAR2}$

Type 8: $k = PAR1*(300/T)^{-PAR2}*\exp(PAR3/T)$.

| | TYPE | PAR1 | PAR2 | PAR3 | REACTIONS |
|---|---|---|---|---|---|
| 27 | 7. | 1.00E-06 | -5.00E-01 | 0.00E+00 | $Na^+.H_2O + E = Na + H_2O$, 7 |
| 28 | 7. | 1.00E-06 | -5.00E-01 | 0.00E+00 | $Na^+.N_2 + E = Na + N_2$, 7 |
| 29 | 7. | 1.00E-06 | -5.00E-01 | 0.00E+00 | $NaO_2^+ + E = NaO_2 +$ , 7 |
| 30 | 1. | 1.00E-10 | 0.00E+00 | 0.00E+00 | $NaO_2^+ + O = NaO^+ + O_2$, 1 |
| 31 | 1. | 5.00E-10 | 0.00E+00 | 0.00E+00 | $NaO^+ + O = Na^+ + O_2$, 1 |
| 32 | 1. | 1.00E-09 | 0.00E+00 | 0.00E+00 | $NaO + O_2+ = NaO^+ + O_2$, 1 |
| 33 | 1. | 1.00E-09 | 0.00E+00 | 0.00E+00 | $NaO + NO^+ = NaO^+ + NO$, 1 |
| 34 | 1. | 4.00E-07 | 0.00E+00 | 0.00E+00 | $NaO^+ + E = Na + O$, 1 |
| 35 | 1. | 6.00E-08 | 0.00E+00 | 0.00E+00 | $Na^+ + [NSUM] = Na + XX$, 1 |
| 36 | 1. | 6.00E-08 | 0.00E+00 | 0.00E+00 | $Na + N_2 + [NSUM] = Na + XX$, 1 |
| 37 | 1. | 6.00E-08 | 0.00E+00 | 0.00E+00 | $Na + CO_2 + [NSUM] = Na + XX$, 1 |
| 38 | 1. | 6.00E-08 | 0.00E+00 | 0.00E+00 | $Na + H_2O + [NSUM] = Na + XX$, 1 |
| 39 | 1. | 6.00E-08 | 0.00E+00 | 0.00E+00 | $NaO^+ + [NSUM] = NaO + XX$, 1 |
| 40 | 1. | 6.00E-08 | 0.00E+00 | 0.00E+00 | $NaO_2^+ + [NSUM] = Na + XX$, 1 |

Table 3

**Calculated Local Topside Scale Heights** (km)

| Altitude (km) | Scale Height† (km) | | | |
|---|---|---|---|---|
| | No ions | K* = 7 x $10^{-31}$†† | K* = 2 x $10^{-31}$ | K* = 4 x $10^{-32}$ |
| 92 | 9.2 | 8.13 | 7.84 | 6.85 |
| 94 | 6.72 | 6.52 | 6.11 | 5.23 |
| 96 | 6.13 | 5.74 | 5.12 | 4.31 |
| 98 | 5.85 | 4.99 | 4.27 | 3.31 |
| 100 | 5.73 | 4.26 | 3.60 | 2.48 |

†Local scale height is obtained from the gradient of Na profile.

††$Na^+ + N_2 + M \rightarrow Na^+ \rightarrow N_2 + M$ with reaction rate $K_S = K^* \left(\frac{300}{T}\right)^{1.5}$. Units for K* are $cm^6\ s^{-1}$.

Experimental Results

Gibson and Sandford (1970): 4 km (98 km), 3 km (100 km), 2 km (102 km).

Megie and Blamont (1977): 2-5 km average scale height above peak.

Simonich et al. (1979): 2.5-5 km at 100 km (scale height changes during night).

References Cited:


Allen, M., J. I. Lunine, and Y. L. Yung (1984) The vertical distribution of ozone in the mesosphere and lower thermosphere. J. Geophys. Res., 89, 4841.

Berger, M. J., S. M. Seltzer, and K. Maeda (1974) Some new results on electron transport in the atmosphere. J. Atmos. Terr. Phys., 36, 591.

Bevilacqua, R. M., J. J. Olivero, P. R. Schwartz, C. J. Gibbins, J. M. Bologna, and D. J. Thacker (1983) An observational study of water vapor in the mid-latitude mesosphere using ground-based microwave techniques. J. Geophys. Res., 88, 8523.

Clemesha, B. R., D. M. Simonich, P. O. Batista, and V. W. J. H. Kirchoff (1982) The diurnal variation of atmospheric sodium. J. Geophys. Res., 87, 181.

Gibson, A. J., and M. C. W. Sandford (1971) The seasonal variation of the night-time sodium layer. J. Atmos. Terr. Phys., 33, 1675.

Goldberg, R. A., and A. C. Aikin (1971) Studies of positive ion composition in the equatorial D region ionosphere. J. Geophys. Res., 76, 8352.

Granier, C., and G. Megie (1982) Daytime Lidar Measurements of the Mesospheric Sodium Layer. Planet. Space Sci. 30, 169.

Hanson, W. B., and J. S. Donaldson (1967) Sodium distribution in the upper atmosphere. J. Geophys. Res.. 72, 5513.

Heimerl, J. M. (1976) Report #1917, U.S.A. Ballistic Research Lab., Maryland.

Hunten, D. M. (1981) A meteor-ablation model of the sodium and potassium layers. Geophys. Res. Lett., 8, 369.

Jegou, J. P., C. Granier, M. L. Chanin, and G. Megie (1984) General theory of the alkali metals present in the Earth's upper atmosphere. I. Transit model: Chemical and dynamical processes. Submitted to Annales de Geophysique.

Kirchoff, V. W. J. H., and P. P. Batista (1983) Calculation of the vertical drift of the sodium ion. Annales Geophysicae, 1, 509.

Krankowsky, D. F., F. Arnold, H. Wider, J. Kissel, and J. Zähringer (1972) Positive ion chemistry in the lower ionosphere. Radio Science, 1, 83.

Megie, G., and J. E. Blamont (1977) Laser sounding of atmospheric sodium: Interpretation in terms of global atmospheric parameters. Planet. Space Sci., 25, 1093.

Murad, E. (1978) Problems in the chemistry of metallic species in the D and E regions. J. Geophys. Res., 83, 5525.

Narcisi, R. S., and A. D. Bailey (1965) Mass spectrometric measurements of positive ions at altitudes from 64 to 112 km. J. Geophys. Res., 70, 3687.

Paulsen, D. E., R. E. Huffman, and J. C. Larrabee (1972) Improved photoionization rates of $O_2(^1\Delta g)$ in the D region. Radio Sci., 7, 51.

Perry, R. A., A. A. Viggiano, D. L. Albritton, E. E. Ferguson, and F. C. Fehsenfeld (1980) Laboratory measurements of stratospheric sodium ion reactions. Geophys. Res. Lett., 7, 693.

Rodriguez, J. M., M. K. W. Ko, and N. D. Sze (1984) The diurnal variation of the neutral sodium species in the upper atmosphere: A model study. Report #AFGL-TR-84-0204, Air Force Geophysics Lab., Bedford, MA., ADA 154988.

Richter, E. S., and C. F. Sechrist, Jr. (1979a) A cluster ion chemistry for the mesospheric sodium layer. J. Atmos. Terr. Phys., 41, 579.

Simonich, D. M., B. R. Clemesha, and V. W. J. H. Kirchoff (1979) The Mesospheric Sodium Layer at 23°S: Nocturnal and Seasonal Variations. J. Geophys. Res. 84, 1543.

Solomon, S., G. C. Reid, D. W. Rusch, and R. J. Thomas (1983b) Mesospheric ozone depletion during the solar proton event of July 13, 1982. Part II: Comparison between theory and measurements. Geophys. Res. Lett., 10, 257.

Strobel, D. F., T. R. Young, R. R. Meier, T. P. Coffey, and A. W. Ali (1974): The nighttime ionisphere: E region and lower F region. J. Geophys. Res., 79, 3171.

Strobel, D. F., C. B. Opal, and R. R. Meier (1980) Photoionization rates in the nighttime E- and F-region ionosphere. Planet. Space Sci., 28, 1027-1033.

Swider, W. (1969a) Processes for meteoric elements in the E region. Planet. Space Sci., 17, 1233-1246.

Swider, W. (1969b) Ionization rates due to the attenuation of 1-100 A nonflare solar X-rays in the terrestrial atmosphere. Rev. Geophys., 7, 573.

Swider, W. (1983) Latitudinal influences on the quiet daytime D region. Adv. Space Res., 2, 213.

Swider, W. (1984) Ionic and neutral concentrations of Mg and Fe near 92 km. Planet. Space Sci., 32, 307.

Swider, W., and W. A. Dean (1975) Effective electron loss coefficient of the disturbed daytime D region. J. Geophys. Res., 80, 1815.

Swider, W., and T. J. Keneshea (1973) Decrease of ozone and atomic oxygen in the lower mesosphere during a PCA event. Planet. Space Sci., 21, 1969-1973.

Swider, W., and R. S. Narcisi (1983) Steady-state model of the D-region during the February 1979 eclipse. J. Atm. Terr. Phys., 45, 493.

Sze, N. D., M. K. W. Ko, R. Specht, and M. Livshits (1980) Modeling of Chemical Processes in the Troposphere and Stratosphere. AFGL-TR-80-0251, Contract No. F 19628-78-C-0215, ADA092704

Torkar, K. M., and M. Friedrich (1983) Tests of an ion-chemical model of the D- and lower E-regions. J. Atm. Terr. Phys., 45, 369.

Torr, D. G., M. R. Torr, R. A. Hoffman, and J. C. G. Walker (1976) Global characteristics of 0.2 to 26 keV charged particles at F region altitudes. Geophys. Res. Lett., 3, 305.

## Figure Captions

Figure 1. Schematic diagram for the chemical scheme of the positive ions in the D and lower E regions. The ions are grouped into two families with $O_2^+$ and $NO^+$ being the primary ions in each group.

Figure 2. Schematic diagram for the chemical scheme of the negative ions in the D and lower E regions.

Figure 3. The production rates for positive ions for daytime and nighttime conditions: A) Day (45° Solar Zenith Angle (SZA)), altitude range 90-120 km); B) Day (45° SZA), altitude range 60-90 km; c) Night (180° SZA), altitude range 60-120 km. An altitude-independent production rate of $10^{-3}$ $cm^3$ $s^{-1}$ due to gallactic x-rays is also included in the model. The curves are: a) x-ray, b) Lyman-β, c) Lyman-α, d) energetic electrons, e) ionization of $O_2(^1\Delta)$, and f) cosmic rays.

Figure 4. Flow chart for the diurnal model of neutral and ionic sodium species.

Figure 5. Calculated diurnal variation of electron density. Profiles are calculated at (a) 86 km, (b) 90 km, (c) 94 km, and (d) 100 km.

Figure 6. Calculated diurnal variation of the densities of $NO^+$ and $O_2^+$. Profiles are calculated at (a) 86 km, (b) 90 km, (c) 94 km, and (d) 100 km.

Figure 7. Calculated total electron and negative ion densities for daytime and nighttime. The positive ion densities are equal to the sum of the electron and the negative ion densities. Curves (a) and (b) are the calculated altitude profiles for electrons for day and night, respectively. The corresponding day and night profiles for the negative ions are given by curves (c) and (d). Curves (e) and (f) are the profiles for electron and negative ions calculated for nighttime including the production of ions from energetic electrons.

Figure 8. Calculated altitude profiles of negative ions for day (A) and night (B). The curves are $O_2^-$ (——), $CO_3^-$ (---), $CO_4^-$ (•••), $NO_3^-$ (-•-•-), $NO_2^-$ (-o-o-), $O^-$ (-Δ-Δ-).

Figure 9. Calculated altitude profiles of $O_2^+$ ("a" for day, "b" for night) and $NO^+$ ("c" for day and "d" for night).

Figure 10. Calculated day (A) and night (B) altitude profiles of the dominant positive ions below 100 km. The curves are $H^+.(H_2O)_4$ (——), $NO^+.(H_2O)$ (---), $NO^+.(H_2O)_2$ (•••), $NO^+.(CO_2)$ (-•-•-), $H^+(H_2O)_3$ (-o-o-).

Figure 11. Schematic diagram for the chemical scheme of sodium neutral and ionic species.

Figure 12. Calculated diurnal variation of the $Na^+$ density at (a) 90 km, (b) 94 km, and (c) 100 km.

Figure 13. Calculated altitude profiles for Na and $Na^+$ at noon.

Figure 14. Calculated altitude profiles of atomic sodium using different rates for reaction (4-4). The curves correspond to values of $K^* = 2 \times 10^{-31}$ $cm^6$ $s^{-1}$ (——), $K^* = 7 \times 10^{-31}$ $cm^6$ $s^{-1}$ (---), $K^* = 4 \times 10^{-32}$ $cm^6$ $s^{-2}$ (-x-), and the case where no $Na^+$ is present (-o-o-).

Figure 15. Calculated profiles of the Na layer, assuming vertical ion drift velocities of 0 (——), -4 (-Δ-Δ-), -10 (-o-o-), and -20 (-x-x-) cm/s.

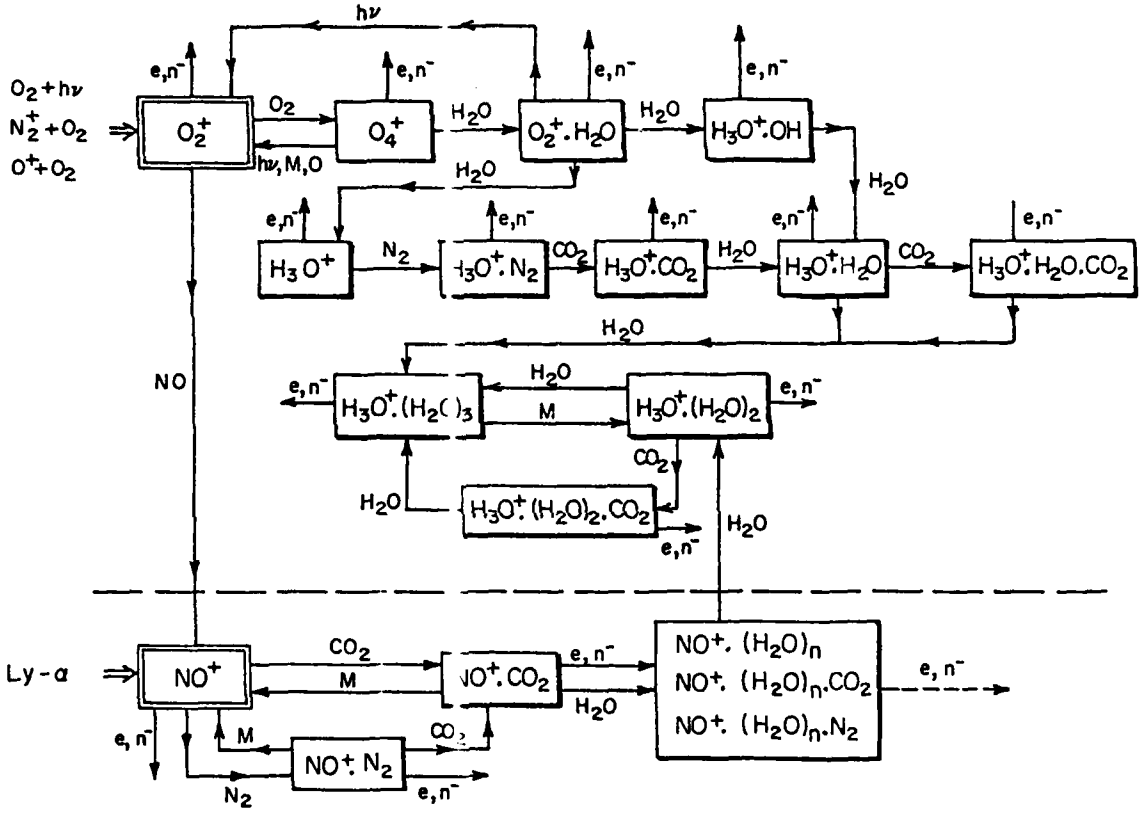


Figure 1. Schematic diagram for the chemical scheme of the positive ions in the D and lower E regions. The ions are grouped into two families with $O_2^+$ and $NO^+$ being the primary ions in each group.

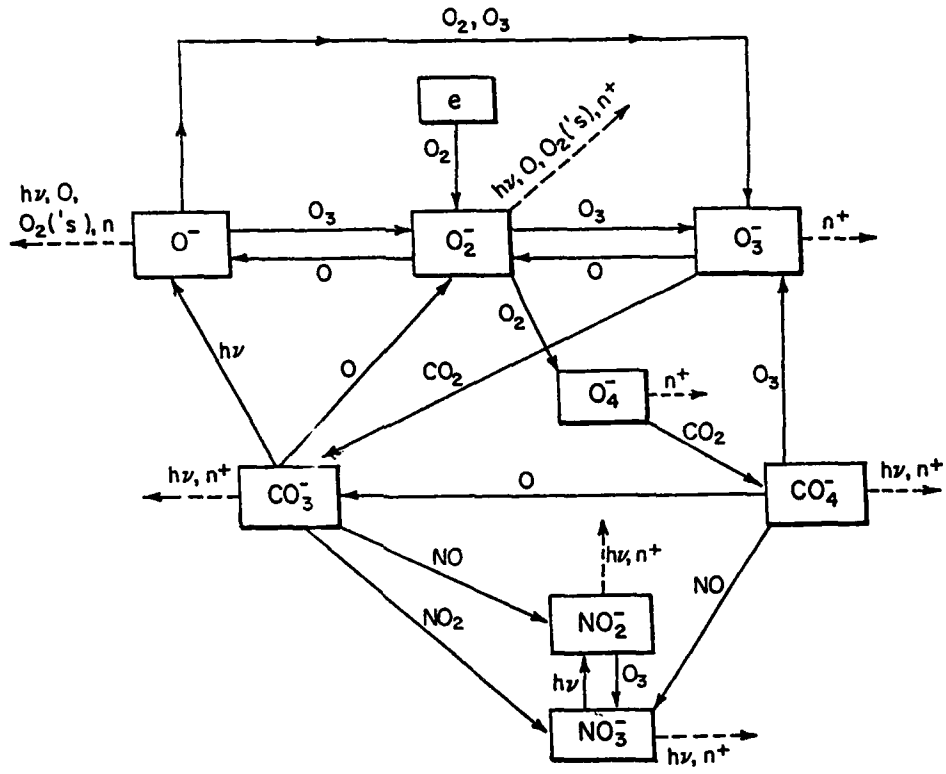


Figure 2. Schematic diagram for the chemical scheme of the negative ions in the D and lower E regions.

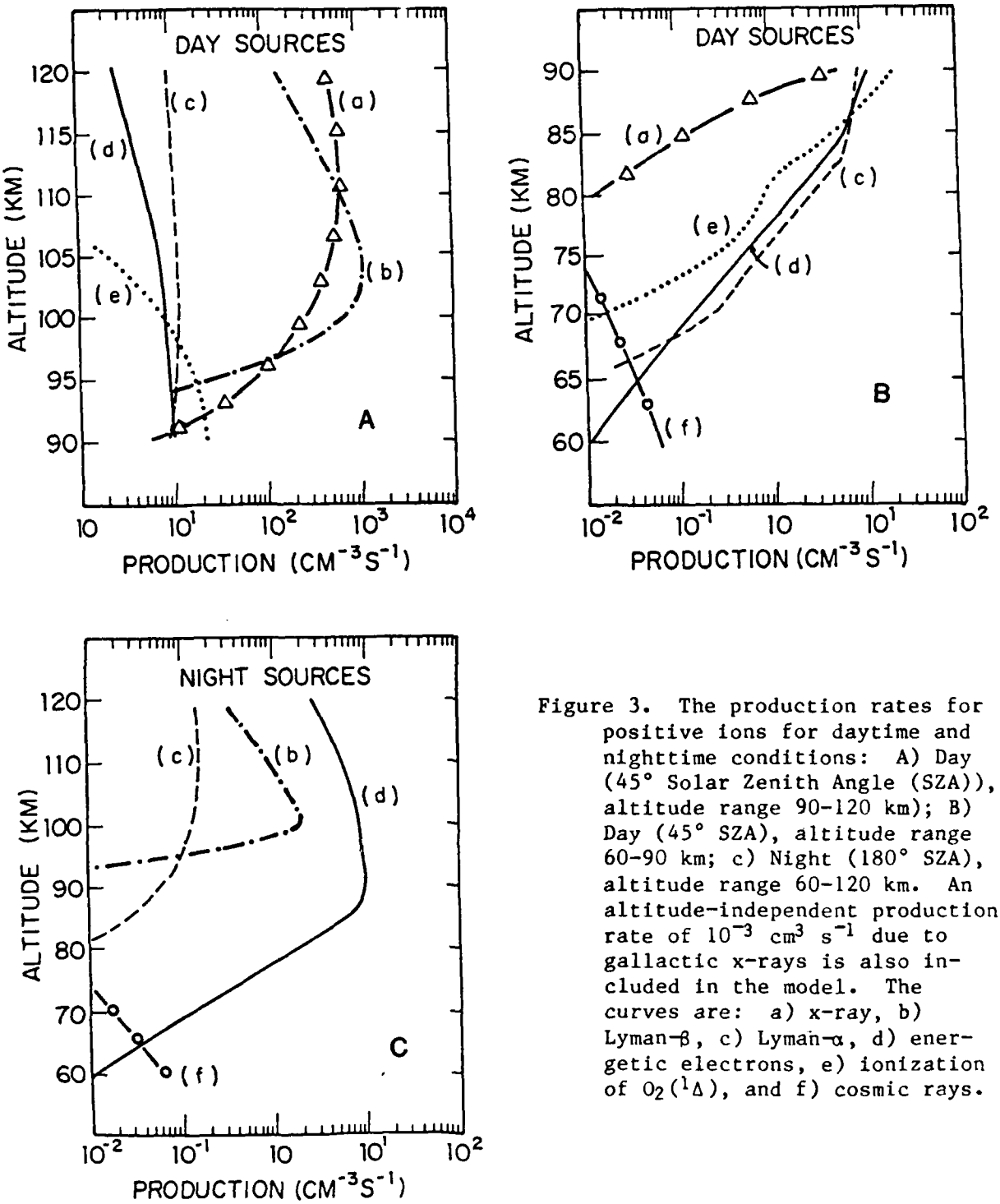


Figure 3. The production rates for positive ions for daytime and nighttime conditions: A) Day (45° Solar Zenith Angle (SZA)), altitude range 90-120 km); B) Day (45° SZA), altitude range 60-90 km; c) Night (180° SZA), altitude range 60-120 km. An altitude-independent production rate of $10^{-3}$ cm$^3$ s$^{-1}$ due to gallactic x-rays is also included in the model. The curves are: a) x-ray, b) Lyman-$\beta$, c) Lyman-$\alpha$, d) energetic electrons, e) ionization of $O_2(^1\Delta)$, and f) cosmic rays.

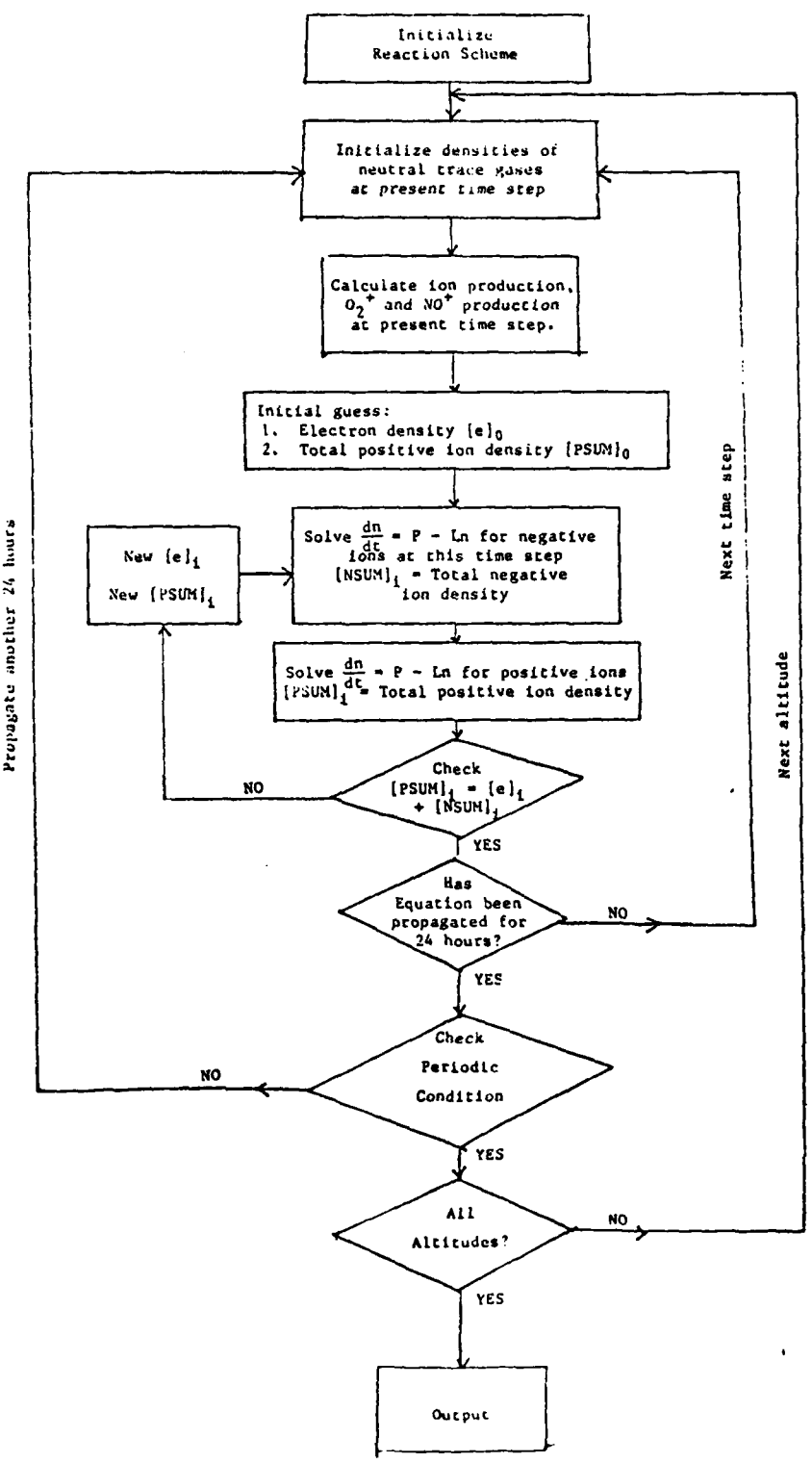


Figure 4. Flow chart for the diurnal model of neutral and ionic sodium species.

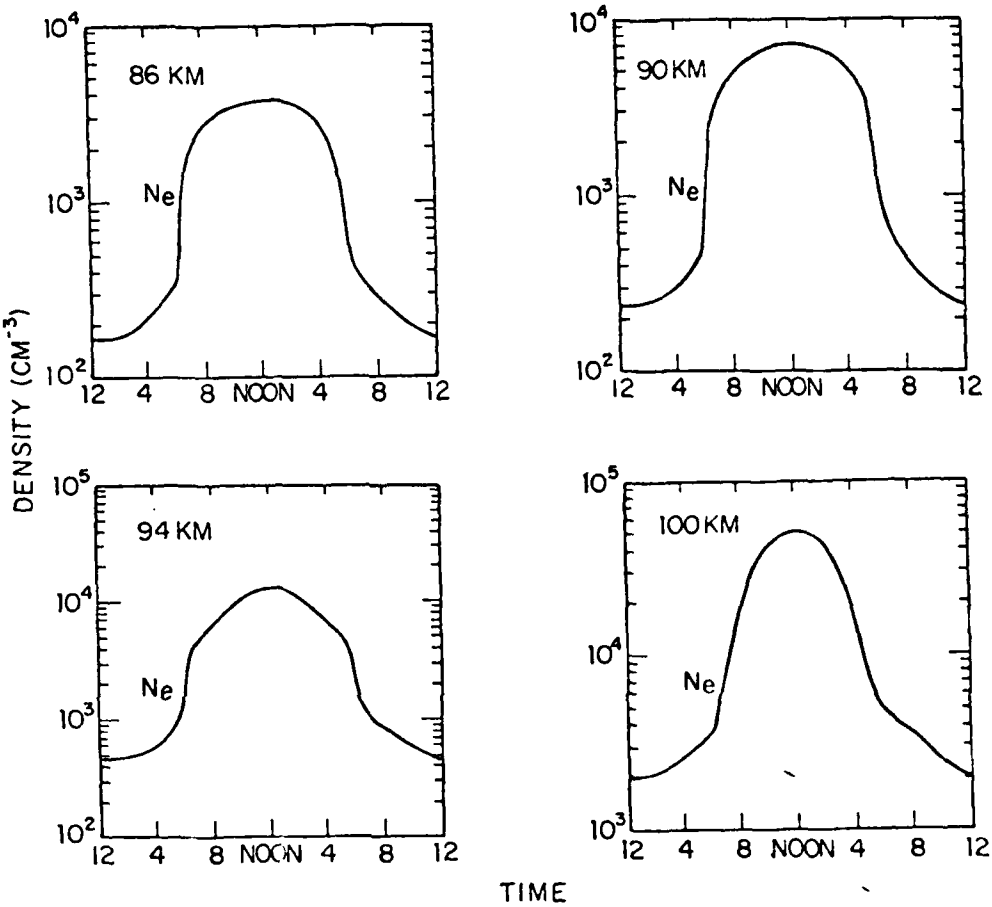


Figure 5. Calculated diurnal variation of electron density. Profiles are calculated at (a) 86 km, (b) 90 km, (c) 94 km, and (d) 100 km.

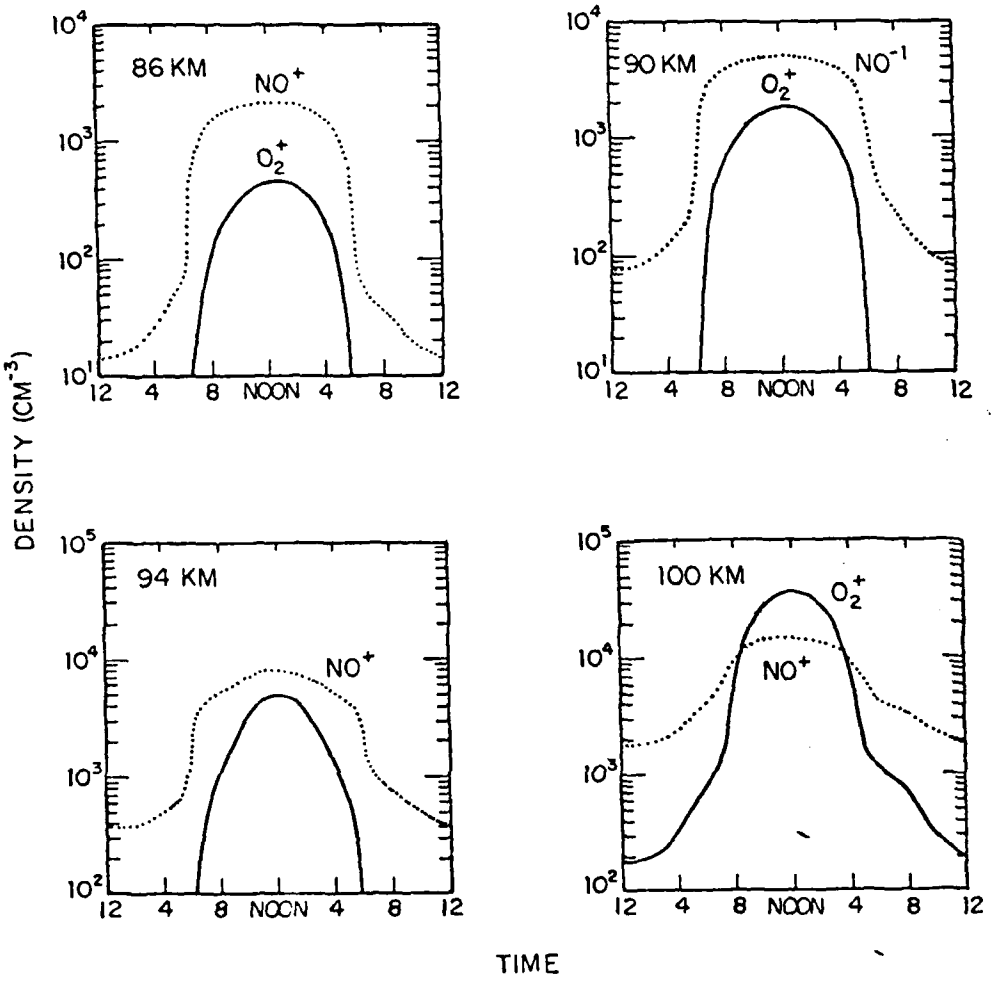


Figure 6. Calculated diurnal variation of the densities of $NO^+$ and $O_2^+$. Profiles are calculated at (a) 86 km, (b) 90 km, (c) 94 km, and (d) 100 km.

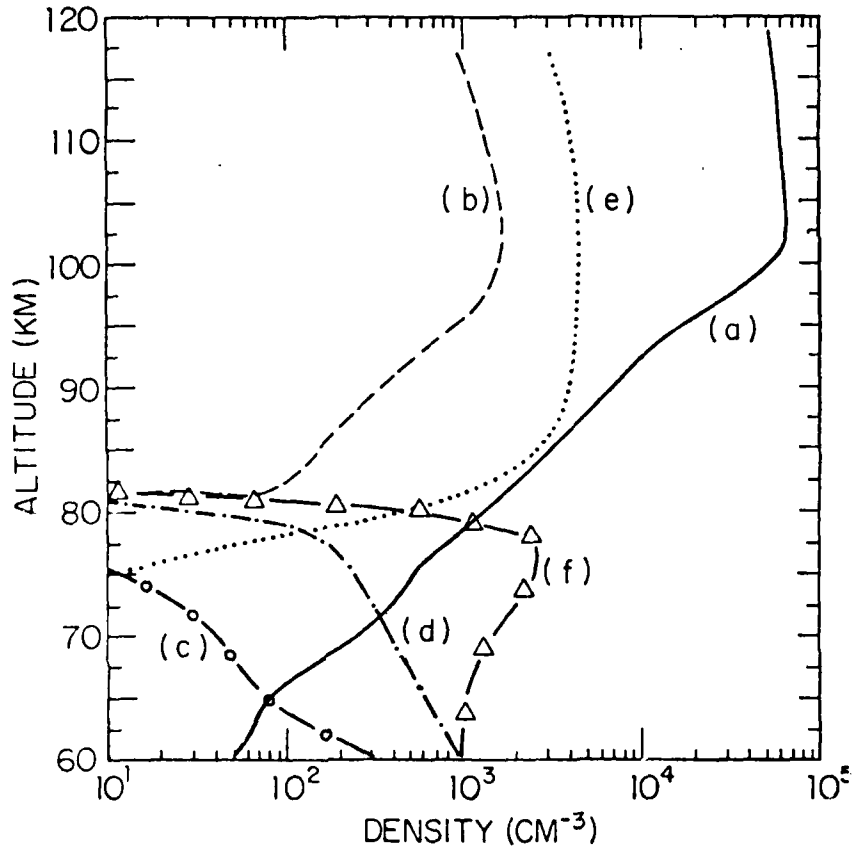


Figure 7. Calculated total electron and negative ion densities for daytime and nighttime. The positive ion densities are equal to the sum of the electron and the negative ion densities. Curves (a) and (b) are the calculated altitude profiles for electrons for day and night, respectively. The corresponding day and night profiles for the negative ions are given by curves (c) and (d). Curves (e) and (f) are the profiles for electron and negative ions calculated for nighttime including the production of ions from energetic electrons.

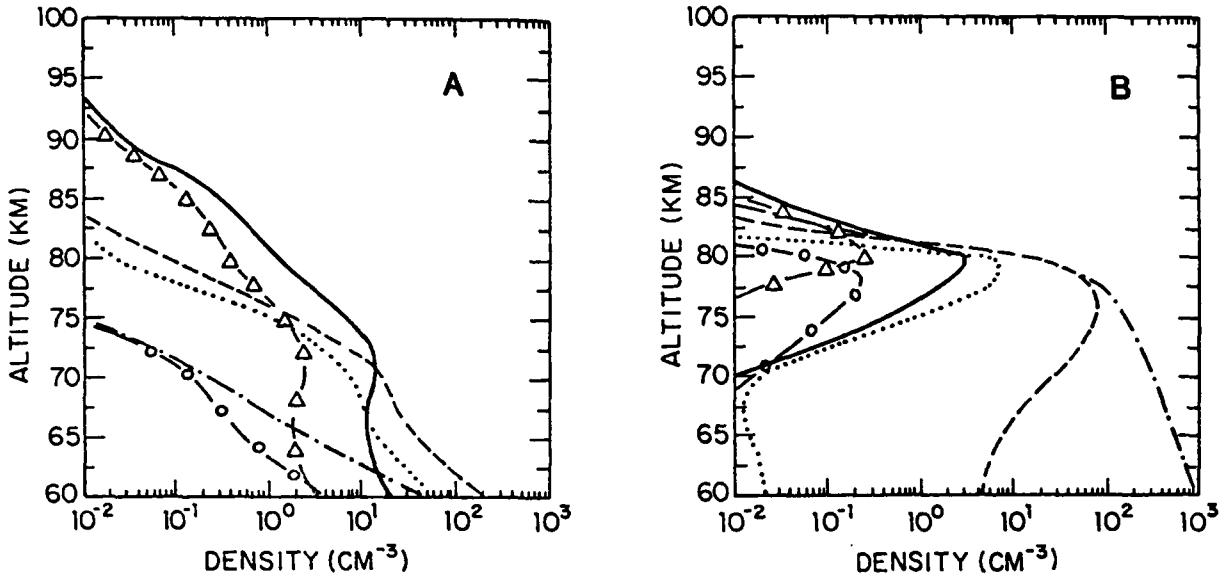


Figure 8. Calculated altitude profiles of negative ions for day (A) and night (B). The curves are $O_2^-$ (——), $CO_3^-$ (---), $CO_4^-$ (•••), $NO_3^-$ (-•-•-), $NO_2^-$ (-o-o-), $O^-$ (-Δ-Δ-).

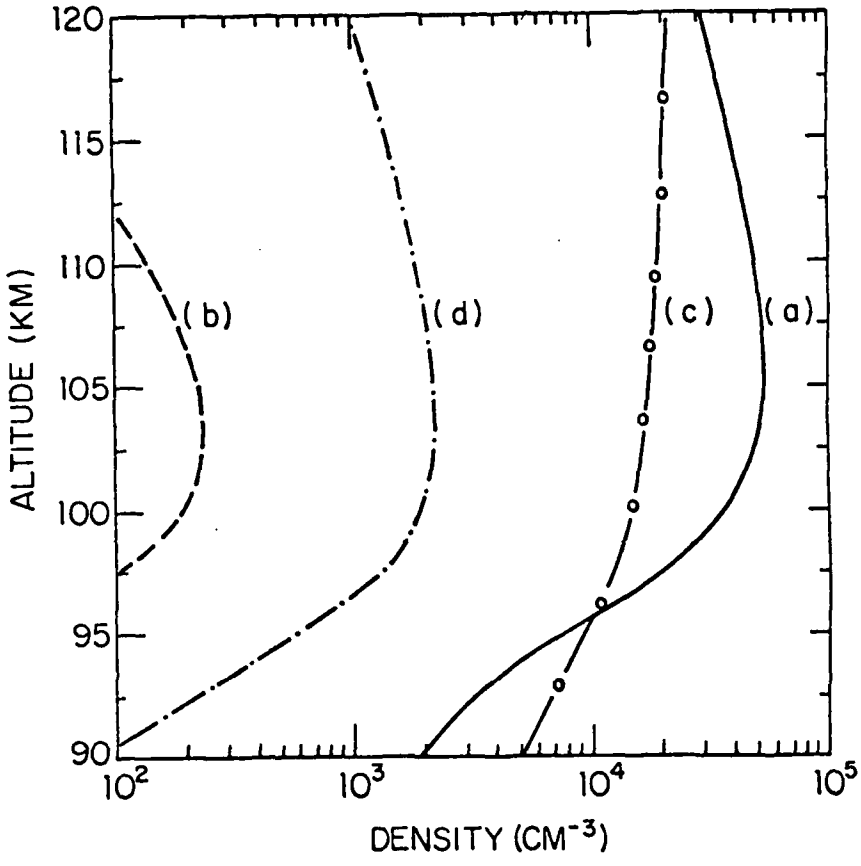


Figure 9. Calculated altitude profiles of $O_2^+$ ("a" for day, "b" for night) and $NO^+$ ("c" for day and "d" for night).

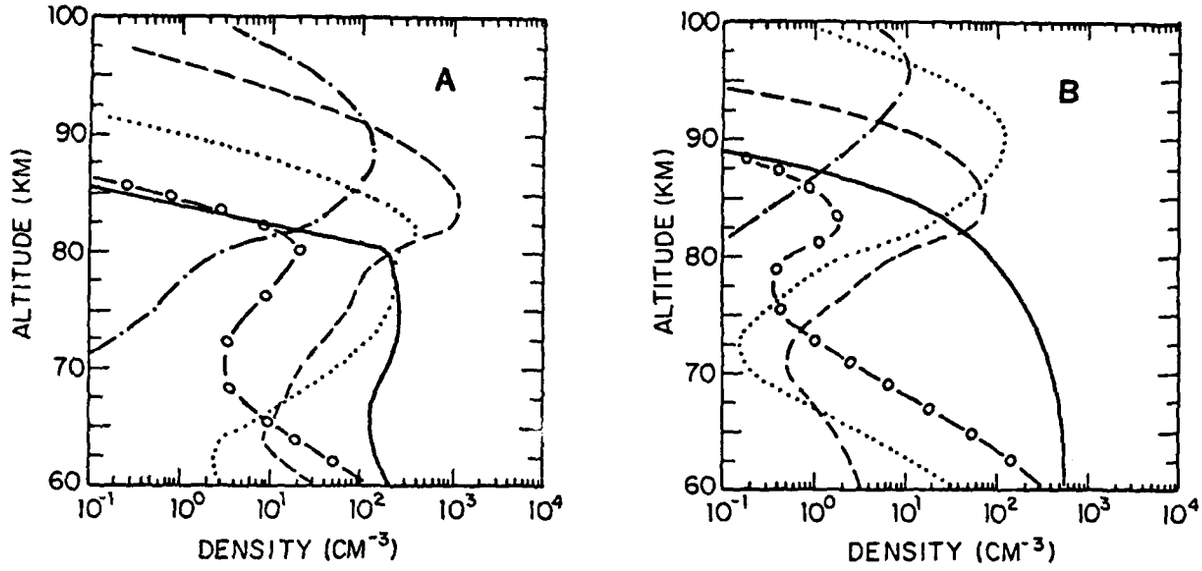


Figure 10. Calculated day (A) and night (B) altitude profiles of the dominant positive ions below 100 km. The curves are $H^+.(H_2O)_4$ (——), $NO^+.(H_2O)$ (---), $NO^+.(H_2O)_2$ (•••), $NO^+.(CO_2)$ (-•-•-), $H^+(H_2O)_3$ (-o-o-).

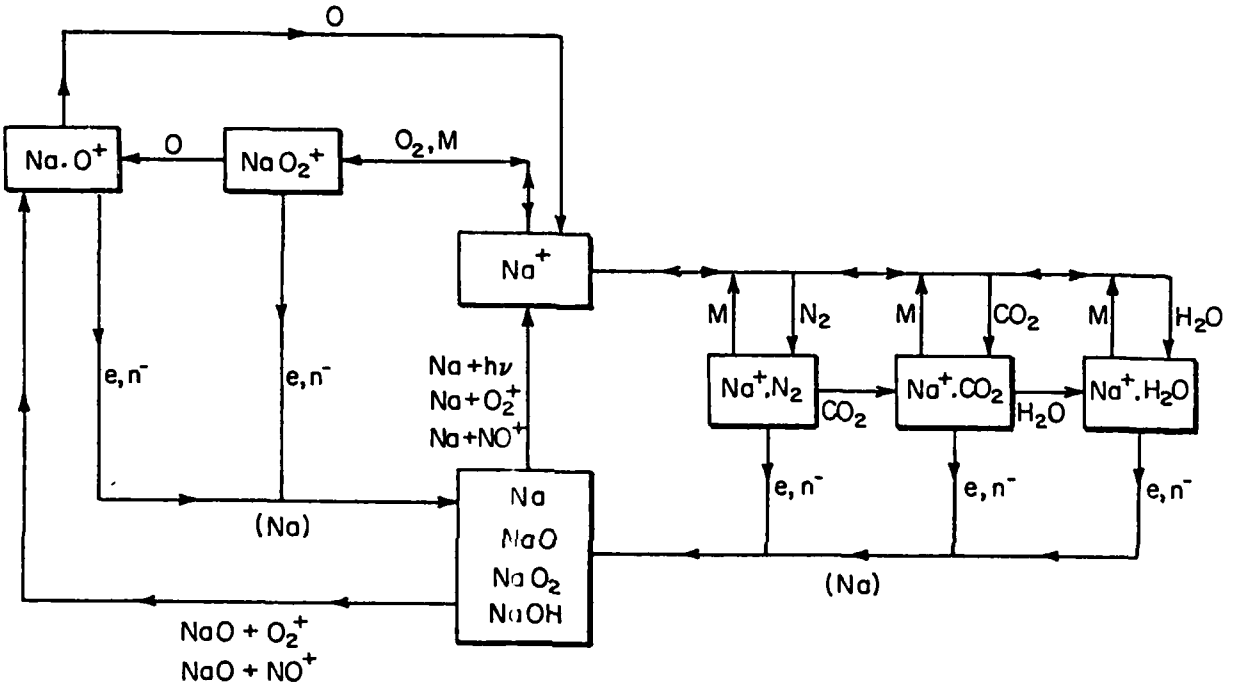


Figure 11. Schematic diagram for the chemical scheme of sodium neutral and ionic species.

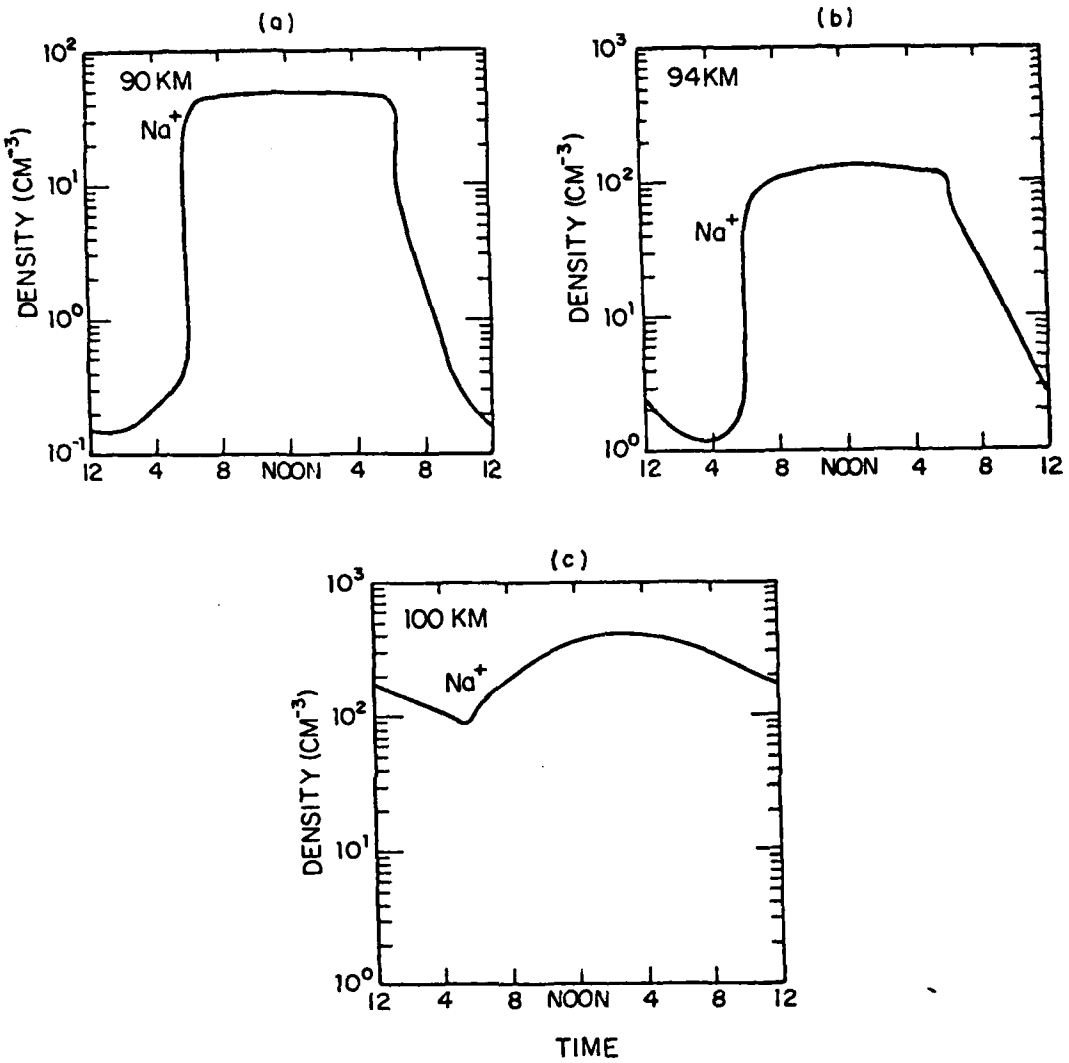


Figure 12. Calculated diurnal variation of the $Na^+$ density at (a) 90 km, (b) 94 km, and (c) 100 km.

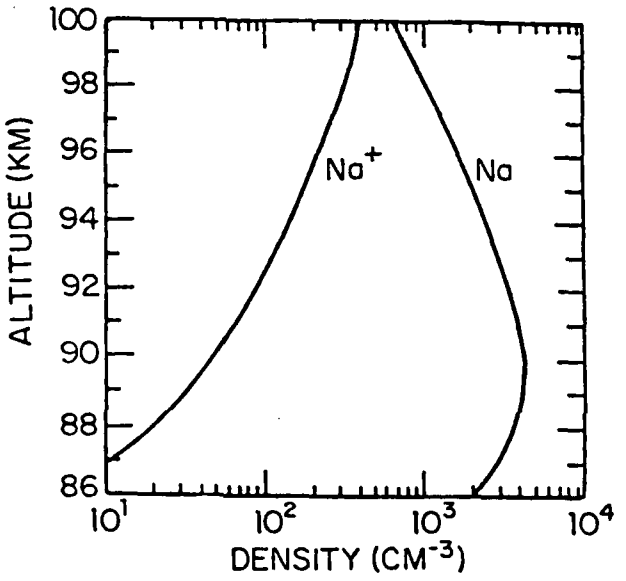


Figure 13. Calculated altitude profiles for Na and $Na^+$ at noon.

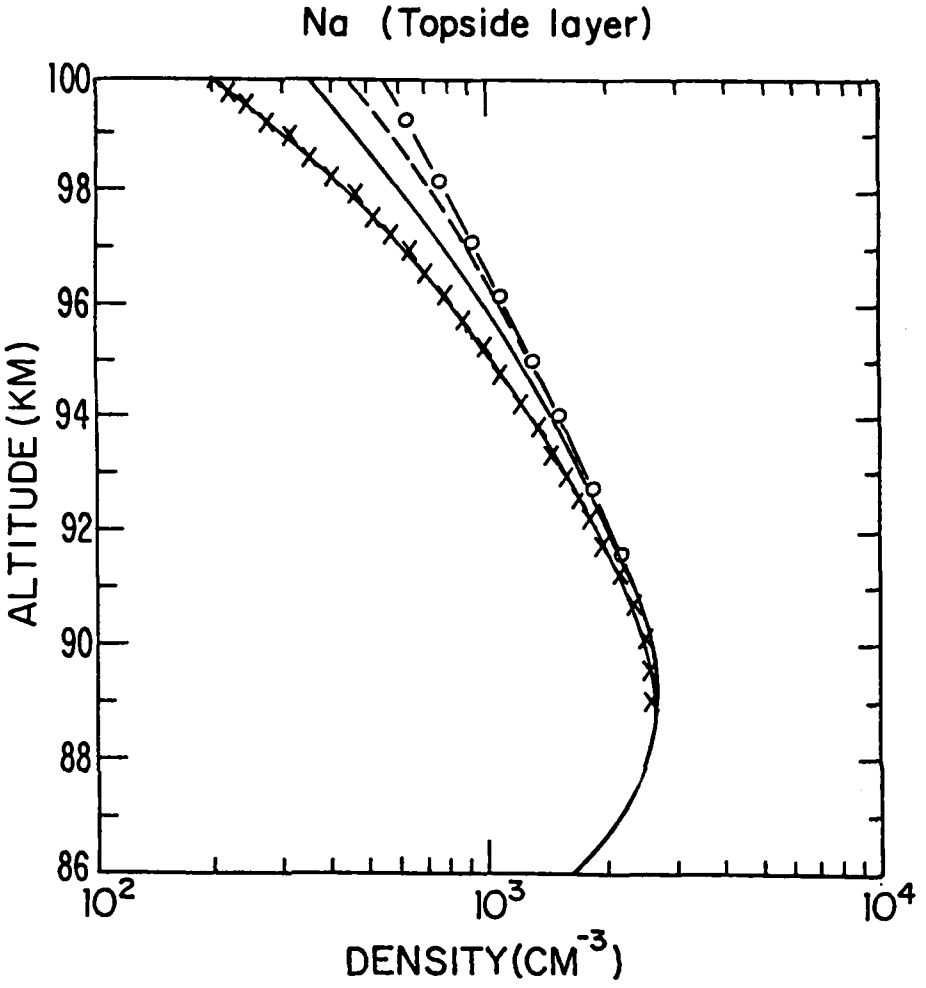


Figure 14. Calculated altitude profiles of atomic sodium using different rates for reaction (4-4). The curves correspond to values of K* = 2 x $10^{-31}$ $cm^6$ $s^{-1}$ (____), K* = 7 x $10^{-31}$ $cm^6$ $s^{-1}$ (---), K* = 4 x $10^{-32}$ $cm^6$ $s^{-2}$ (-x-), and the case where no $Na^+$ is present (-o-o-).

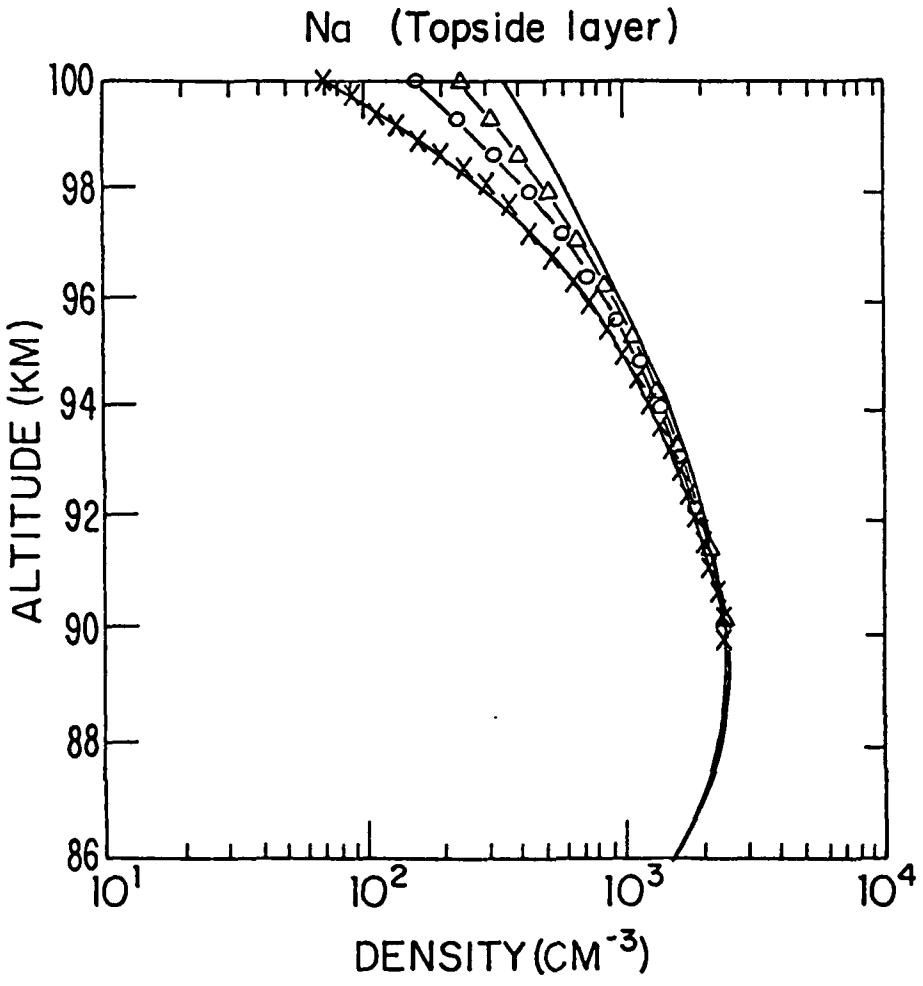


Figure 15. Calculated profiles of the Na layer, assuming vertical ion drift velocities of 0 (——), -4 (-Δ-Δ-), -10 (-o-o-), and -20 (-x-x-) cm/s.

PART B

Impact of Neutral Sodium Chemistry on the Stratospheric Chlorine Cycle

Recent theoretical and experimental developments in sodium chemistry have created much interest in its role in stratospheric chlorine chemistry. Murad, Swider, and Benson (1981) first suggested that the reaction

$$*\text{R19:} \qquad \text{NaOH} + \text{HCl} \xrightarrow{k_{19}} \text{NaCl} + \text{H}_2\text{O}$$

would provide a favored pathway for removal of NaOH in competition with NaOH photolysis if $k_{19} > 10^{-11}$ cm$^3$ s$^{-1}$. If NaCl does not react to release the Cl atoms, R19 could be an important sink for stratospheric chlorine species if the atmospheric concentration of total sodium (NaX) is sufficiently high.

On the other hand, Rowland and Rogers (1982) suggested that NaCl could be rapidly photolysed based on the assumption of unity quantum yield and the absorption cross sections measured at high temperatures. Reaction R19, followed by

$$\text{R20:} \qquad \text{NaCl} + h\nu \xrightarrow{J_{20}} \text{Na} + \text{Cl}$$

could then provide an additional mechanism for converting HCl to Cl, similar to the well-known source

$$\text{OH} + \text{HCl} \xrightarrow{k_A} \text{H}_2\text{O} + \text{Cl} \qquad (1)$$

at altitudes below 50 km.

Subsequent measurements by Silver et al. (1984) have obtained values of $2.5 \times 10^{-10}$ cm$^3$ s$^{-1}$ for reaction R19. This reaction will affect the partitioning of the chlorine species in the upper stratosphere when

---

*Reaction numbers R_ and rates k_, J_, refer to the reactions in Table 1.

$$J_{20}\ [NaCl] \sim k_A[OH][HCl]. \qquad (2)$$

If $R_{19}$ is the only mechanism for forming NaCl, (2) reduces to

$$k_1\ [NaOH] \sim k_A[OH] \qquad (3)$$

which translates into

$$[NaOH] \sim 10^4\ cm^{-3} \qquad (4)$$

for typical stratospheric concentration of $10^6\ cm^{-3}$ for OH.

The density of sodium species NaX (Na, NaO, $NaO_2$, NaOH, NaCl) in the lower stratosphere is $\sim 10^5\ cm^{-3}$, if one assumes that sodium diffuses down from the mesosphere and is removed in the troposphere with a time constant of ten days (Liu and Reid, 1979; Sze et al., 1982). In the stratosphere, most of the NaX is expected to be in the form of $NaO_2$ and NaOH. Past attempts in assessing the impact of Na on stratospheric chlorine chemistry were hampered by the lack of kinetic data to determine the NaOH concentration in the stratosphere.

Recent measurements reported by Silver and Kolb (1985) indicated a rate of $2 \times 10^{-10}\ cm^3\ s^{-1}$ for the reaction

R21: $NaO_2 + HCl \rightarrow NaCl + HO_2$.

Since both NaOH and $NaO_2$ react with HCl at about the same rate, the partitioning between the two reservoirs is no longer crucial. Indeed, the concentration of NaCl in the stratosphere can be estimated from the total sodium concentrations via the following set of algebraic equations:

$$J_{20}[NaCl] = k^*[HCl][NaR] \quad (5a)$$

$$[NaCl] + [NaR] \cong [NaX] \quad (5b)$$

where [NaR] is the sum of [NaOH] and [$NaO_2$], and $k^* = 2 \times 10^{-10}$ $cm^3$ $s^{-1}$ is the reaction rate constant for $NaO_2$ and NaOH with HCl. Equation (5a) follows from the photochemical equilibrium assumption for NaCl while equation (5b) follows from the closure relationships assuming that [Na]/[NaX] and [NaO]/[NaX] $\ll 1$. From equations (5), it follows that

$$[NaCl] = \frac{k^*[HCl][NaX]}{J_{20} + k^*[HCl]}. \quad (6)$$

In the stratosphere ($Z < 50$ km) with [HCl] $\sim 10^8$ $cm^{-3}$, $k^*$[HCl] $\sim 10^{-2}$ $s^{-1}$. As long as $J < k^*$[HCl], the sodium species will be in the form of NaCl. Thus, the effectiveness of R20 in recycling HCl to Cl will be linear in $J_{20}$ and [NaX].

Our present knowledge of the reactions controlling sodium chemistry is summarized in Table 1. The photolysis rates for NaCl and NaOH (reactions R20 and R4), estimated by Rowland and Rogers (1982) and Rowland and Makide (1982) can be considered only upper bounds to the actual rates. Rates for other reactions are usually estimated from analogy to similar reactions involving H instead of Na. Observations of the properties of the mesospheric sodium layer and the sodium D-line nightglow are used to constrain the rate for reactions R2, R5, and R6 (Bates and Ojha, 1980; Rodriguez, Ko, and Sze, 1984).

We will now present some quantitative results using our stratospheric model. The value adopted for $J_{20}$ in the model is shown in Figure 1 and is similar to those suggested by Rowland and Rogers (1980). Figure 2 shows the calculated profiles for $NaO_2$, NaOH, and NaCl. Figure 3 compares the rate of

recycling HCl to Cl by photolysis of NaCl with the reaction of OH + HCl. The calculated conversion rate is linear in the $J_{20}$ and [NaX] in the lower stratosphere, and the mechanism could dominate the OH + HCl reaction if $J_{20}$ is sufficiently fast (i.e., $J_{20} \sim 10^{-3}$ $s^{-1}$).

Note that the above calculation should be considered as the upper limits since heterogeneous reactions involving NaCl, or dimerization (Lamb and Benson, 1985), may prevent it from photolysing. In addition, reaction of NaOH with other species may prevent formation of NaCl. One possibility was suggested by Murad and Swider (1979) where NaOH reacts with $CO_2$ to form $NaHCO_3$:

$$NaOH + CO_2 \xrightarrow{M} NaHCO_3.$$

Estimated reaction rate is $\sim 10^{-32}$ $cm^6$ $s^{-1}$, giving a loss frequency for NaOH of about $2 \times 10^{-2}$ $s^{-1}$, .475 $s^{-1}$, and 10 $s^{-1}$, at 40 km, 30 km, and 20 km respectively. If the reaction indeed proceeds at this rate, all the sodium species will be in the form of $NaHCO_3$.

Although there are large uncertainties in the sodium chemistry, the following statements can be established. Given the stratospheric chlorine concentration of about $10^8$ to $10^9$ $cm^{-3}$, the present estimated concentration of $10^5$ $cm^{-3}$ for NaCl will not constitute an important reservoir for chlorine. Any impact on the chlorine cycle must then involve a catalytic mechanism. Our calculation shows that if gaseous NaCl is the major sodium compound and $J_{20} > 10^{-3}$ $s^{-1}$, photolysis of NaCl will be an important pathway for cycling HCl to Cl in the stratosphere. However, the calculation did not take into consideration the possibility of the formation of other sodium compounds such as $NaHCO_3$, $(NaCl)_n$, or incorporation of NaCl into aerosols.

Table 1: Reaction Scheme and Rate Constants

| | Reaction | Rate[a] |
|---|---|---|
| 1. | $Na + O_3 \rightarrow NaO + O_2$ | 3.5(-10) [h] |
| 2. | $NaO + O \rightarrow Na\ (^2P, ^2S) + O_2$ | 4(-11) [c] |
| 3. | $Na + O_2 + N_2 \rightarrow NaO_2 + N_2$ | $1.9 \times 10^{-30}(T/300)^{-1.1}$ [d] |
| 4. | $NaOH + h\nu \rightarrow Na + OH$ | 2(-3) [e] |
| 5. | $NaO_2 + h\nu \rightarrow Na + O_2$ | 1(-4) [c] |
| 6. | $NaO_2 + O \rightarrow NaO + O_2$ | 1(-13) [c] |
| 7. | $NaO + H_2O \rightarrow NaOH + OH$ | 2(-10) [i] |
| 8. | $NaO + O_3 \rightarrow NaO_2 + O_2$ | 1.8(-10) [i] |
| 9. | $NaO + H \rightarrow Na + OH$ | 1(-14) [g] |
| 10. | $NaO_2 + OH \rightarrow NaOH + O_2$ | 1(-11) [f] |
| 11. | $NaO_2 + H \rightarrow NaOH + O$ | 1(-13) [g] |
| 12. | $NaOH + H \rightarrow Na + H_2O$ | 1.4(-12) [f] |
| 13. | $NaOH + (^1D) \rightarrow NaO + OH$ | 1(-10) [g] |
| 14. | $Na + HO_2 \rightarrow NaOH + O$ | 1(-10) [f] |
| 15. | $NaO + O_3 \rightarrow Na + 2O_2$ | 1(-10) [i] |
| 16. | $NaO + HO_2 \rightarrow NaOH + O_2$ | 1(-11) [f] |
| 17. | $NaO + H_2 \rightarrow Na + H_2O$ | 1(-11) [i] |
| 18. | $NaO + H_2 \rightarrow NaOH + H$ | 2.6(-11) [i] |
| 19. | $NaOH + HCl \rightarrow NaCl + H_2O$ | 2.5(-10) [d] |
| 20. | $NaCl + h\nu \rightarrow Na + Cl$ | $J < 6(-2)$ [j] |
| 21. | $NaO_2 + HCl \rightarrow NaCl + HO_2$ | 2.5(-10) [k] |

[a]Read 3(-10) as $3 \times 10^{-10}$. Units are $cm^3\ s^{-1}$, except $cm^6\ s^{-1}$ for (3) and $s^{-1}$ for (4), (5), and (15). [b] Kolb and Elgin (1976); [c] Sze et al. (1982); [d] Silver et al. (1984); [e] Rowland and Makide (1982); [f] Liu and Reid (1979); [g] Kirchoff and Clemesha (1983); [h] Zahniser et al. (1985); [i] Ager and Howard (1985); [j] Rowland and Roger (1982); [k] Silver and Kolb (1985).

References Cited:


Ager, Joel W., III, and C. J. Howard (1985) Kinetic studies of some sodium reactions of atmospheric importance. EOS, 66, 317.

Bates, D. R., and P. C. Ojha (1980) Excitation of the Na D-doublet of the nightglow. Nature, 286, 790.

Kirchoff, V. W. J. H., and B. R. Clemesha (1983) The atmospheric neutral sodium layer, 2. Diurnal variations, J. Geophys. Res., 88, 442.

Kolb, C. E., and J. B. Elgin (1976) Gas phase chemical kinetics of the Na in the upper atmosphere, Nature, 263, 488.

Lamb, J. J., and S. W. Benson (1985) Possible fates of sodium in the atmosphere. EOS, (66), 317

Liu, S. C., and G. C. Reid (1979) Sodium and other minor constituents of meteoric origin in the atmosphere. Geophys. Res. Lett., 6, 283.

Murad, E., and W. Swider (1979) Chemistry of meteor metals in the stratosphere. Geophys. Res. Lett., 6, 929.

Murad, E., W. Swider, and S. W. Bensen (1981) Possible role for metals in stratospheric chlorine chemistry. Nature, 289, 273.

Rodriguez, J. M., M. K. W. Ko, and N. D. Sze (1984) The diurnal variation of the neutral sodium species in the upper atmosphere: A model study. Report #AFGL-TR-84-0204, Air Force Geophysics Lab., Bedford, MA., ADA 154988.

Rowland, F. S., and Y. Makide (1982) Upper stratospheric photolysis of NaOH. Geophys. Res. Lett., 9, 473-475.

Rowland, F. S., and P. J. Rogers (1982) Upper stratospheric photolysis of NaCl and KCl. Proc. Nat. Acad. Sci. USA, 79, 2737.

Silver, J. A., and C. E. Kolb (1985) Stratospheric chemistry of meteoric metals: Measurements of the rate constant for $NaO_2$ + HCl and the photodissociation cross sections for NaCl. EOS, 66, 317.

Silver, J. A., M. S. Zahniser, A. C. Stanton, and C. E. Kolb (1984) Temperature-dependent termolecular reaction rate constants for potassium and sodium peroxide formation. Presented at the 20th International Symposium on Combustion, the Combustion Institute, Pittsburgh, PA.

Sze, N. D., M. K. W. Ko, W. Swider, and E. Murad (1982) Atmospheric Sodium Chemistry. I. The Altitude Region 70-100 km. Geophys. Res. Lett., 9, 1187-1190.

Zahniser, M. S., J. A. Silver, and C. E. Kolb (1985) Mesospheric chemistry of meteoric metals: Reaction rate measurements for Na + $O_3$. EOS, 66, 317.

## Figure Captions

Figure 1. Photolysis rate of NaCl used in the model calculation. The values are taken from Rowland and Rogers (1982).

Figure 2. Calculated concentrations of the sodium species in the stratosphere. The concentrations of Na and NaO are less than 10 $cm^{-3}$ in the lower stratosphere.

Figure 3. Comparison of the conversion rate of HCl to Cl by NaCl photolysis (——) and reaction OH + HCl (---).

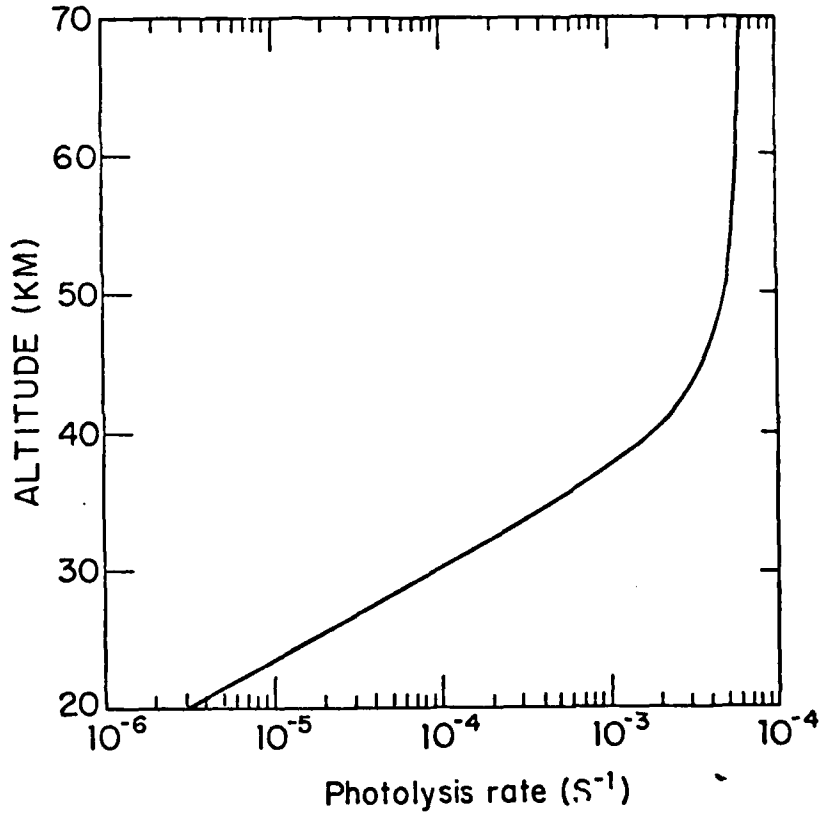


Figure 1. Photolysis rate of NaCl used in the model calculation. The values are taken from Rowland and Rogers (1982).

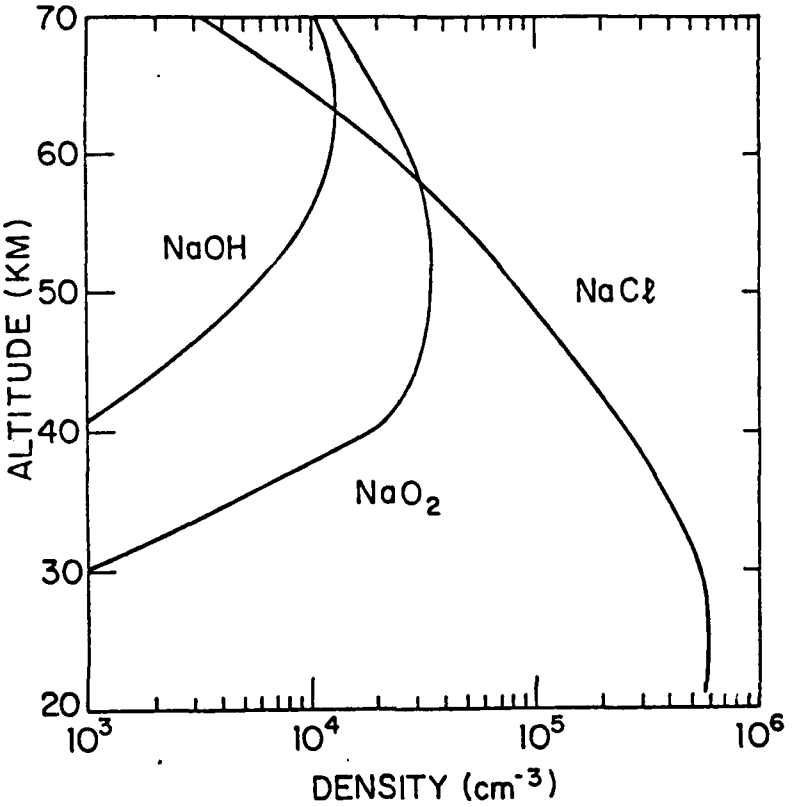


Figure 2. Calculated concentrations of the sodium species in the stratosphere. The concentrations of Na and NaO are less than 10 $cm^{-3}$ in the lower stratosphere.

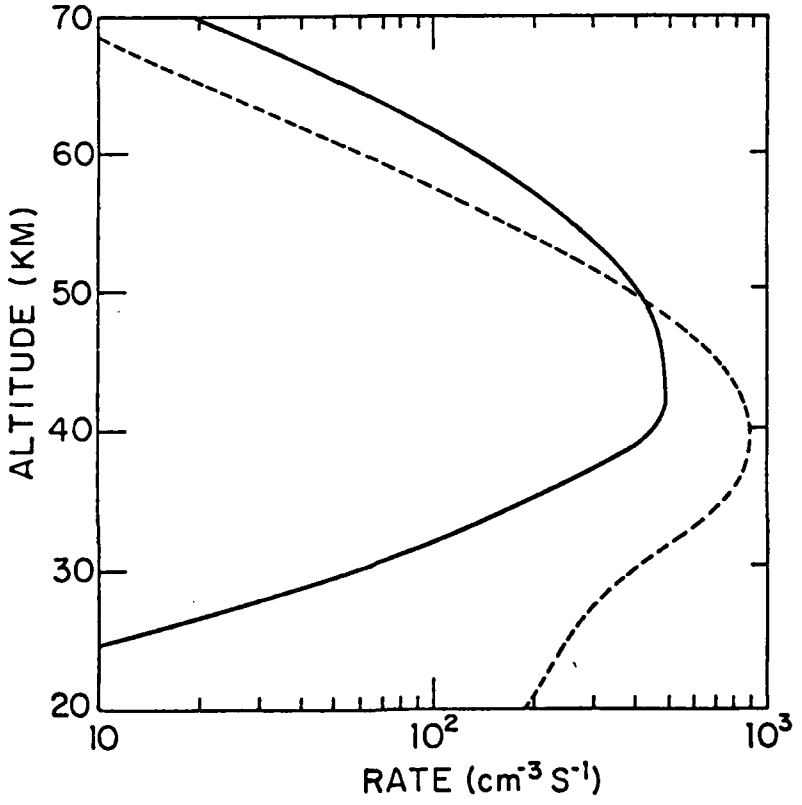


Figure 3. Comparison of the conversion rate of HCl to Cl by NaCl photolysis (——) and reaction OH + HCl (---).

DTIC

END

4-86